Title

MEASUREMENT OF RADIATIVE LIFETIMES. I: AN APPARATUS FOR MEASUREMENT OF MILLIMICROSECOND RADIATIVE LIFETIMES OF GAS-PHASE MOLECULES. II: THE RADIATIVE LIFETIMES OF THE BO^ STATE OF I2 BY TWO ABSOLUTE ABSORPTION METHODS.

Author

Stafford, Fred Ezra.

Publication Date

1959-09-21

UCRL 8854

UNIVERSITY OF CALIFORNIA

Ernest O. Lawrence

Radiation Laboratory

MEASUREMENT OF RADIATIVE LIFETIMES

I. AN APPARATUS FOR MEASUREMENT OF MILLIMICROSECOND RADIATIVE LIFETIMES OF GAS-PHASE MOLECULES

II. THE RADIATIVE LIFETIME OF THE $B\,O_u^+$ STATE OF I_2 BY TWO ABSOLUTE ABSORPTION METHODS

APPENDIX: DESCRIPTION OF ELECTRONIC SYSTEM

DISCLAIMER

UCRL-8854
Chemistry-General
TID-4500(15th Ed.)

UNIVERSITY OF CALIFORNIA

Lawrence Radiation Laboratory
Berkeley, California

Contract No. W-7405-eng-48

MEASUREMENT OF RADIATIVE LIFETIMES

I. AN APPARATUS FOR MEASUREMENT OF MILLIMICROSECOND RADIATIVE LIFETIMES OF GAS-PHASE MOLECULES.

II. THE RADIATIVE LIFETIME OF THE B 0_u^+ STATE OF I_2 BY TWO ABSOLUTE ABSORPTION METHODS

Fred Ezra Stafford

(Thesis)

APPENDIX: DESCRIPTION OF ELECTRONIC SYSTEM

Jerry M. Sakai and Fred E. Stafford

September 21, 1959

Printed for the U. S. Atomic Energy Commission

Printed in USA. Price $2.75. Available from the
Office of Technical Services
U. S. Department of Commerce
Washington 25, D.C.

MEASUREMENT OF RADIATIVE LIFETIMES

Contents

I. AN APPARATUS FOR MEASUREMENT OF MILLIMICROSECOND RADIATIVE LIFETIMES OF GAS-PHASE MOLECULES

MEASUREMENT OF RADIATIVE LIFETIMES

II. THE RADIATIVE LIFETIME OF THE B 0_u^+ STATE OF I_2 BY TWO ABSOLUTE ABSORPTION METHODS

MEASUREMENT OF RADIATIVE LIFETIMES

APPENDIX

DESCRIPTION OF ELECTRONIC SYSTEM

MEASUREMENT OF RADIATIVE LIFETIMES

Fred Ezra Stafford

(Thesis)

Lawrence Radiation Laboratory and Department of Chemistry
University of California, Berkeley, California

September 21, 1959

ABSTRACT

I. AN APPARATUS FOR MEASUREMENT OF MILLIMICROSECOND RADIATIVE LIFETIMES OF GAS-PHASE MOLECULES

Knowledge of radiative lifetimes is valuable for application to problems in thermodynamics of high-temperature systems, kinetics of energy transfer, and electronic structure of molecules. Although measurement of these lifetimes involves working with millimicrosecond times and extremely low signal levels, various methods have been developed and are summarized.

The instrument described here measures a change in phase produced by the finite time required for fluorescence. Exciting light is 65% modulated at 5.2 Mc by a supersonic grating modulator. The 5.2-Mc fluorescence signal is beat to 1000 $\pm$ .1 cps, and its phase is measured by the use of calibrated phase shifters and a null-indicating phase detector. The phase detector has a long time constant which causes it to "average out" much of the noise that reaches it.

The accuracy and sensibility of the instrument for low-level signals are limited by the phase-detector sensibility of $\pm$ 0.5°. With the present frequency of modulation, lifetimes between 6×10^{-9} and 10^{-7} sec can be measured within 20%. Measurement of the time of flight of light shows that absolute accuracy is within this sensibility.

II. THE RADIATIVE LIFETIME OF THE B 0_u^+ STATE OF I_2 BY TWO ABSOLUTE ABSORPTION METHODS

The lifetime of the level of iodine which combines with the ground state to give rise to the visible-band system is determined to be 5×10^{-7} sec $\pm$ 20% from measurements of the integrated band absorption. This state has been assigned the designation B 0_u^+. The value 3×10^{-7} sec is obtained from absorption of a single line plus relative intensities of only the first 18 members of the fluorescence series and is much more uncertain. Consideration of the sum rules for transition probability leads to the expectation that variation of electronic-transition probability over the band system is not large, and that the average value obtained from the total band absorption measurements should be valid for $v' = 26$ in particular. However, the lifetime may be up to 30% longer than the value stated because of the energy-cubed dependence of the fluorescence rate and the extension of the fluorescence series far into the red.

Various data for vibrational-energy transfer and for quenching of the B 0_u^+ $v' = 26$, $J' = 34$ level are put on an absolute scale with this lifetime. The cross section for collisions with various gases to produce vibrational transfer to states with $v' = 24$, 25, or 27 ranges between 1/3 and 1/13 of the gas kinetic cross section. The cross section for quenching by foreign gases ranges between 1 and 1/30, while that for self-quenching is 3 times the gas kinetic cross section.

List of Symbols Used

Part I

BW	Bandwidth
f	Frequency of modulation
	Also, oscillator strength
	Also, optical focal ratio
g	Statistical weight
I	Light intensity
J	Rotational quantum number
k	Rate constant
Θ	Phase shift produced by electronic phase shifter
λ	Wavelength
ν	Vibrational quantum number
ξ	Phase difference between reference and sample signals at detector
τ	Lifetime
ϕ	Phase shift due to lifetime of molecular species
ω	Angular frequency

I. AN APPARATUS FOR MEASUREMENT OF MILLIMICROSECOND RADIATIVE LIFETIMES OF GAS-PHASE MOLECULES.

A. INTRODUCTION

Knowledge of radiative lifetimes of gas-phase molecules is of interest for many reasons. However, both the signal levels available and the range of lifetimes have made searching for this knowledge an extremely difficult problem. Although lifetime measurements have been made previously, the equipment, dating back over 30 years, has been designed primarily for measurements on solutions.

The main endeavor of the present work has been to make feasible measurements of extremely small signals from gas-phase molecules. Salient features of the present instrument are the supersonic-grating light modulator, precise frequency control, precision electrical phase shifter, and phase-detector indicator with long time constant to average over random noise fluctuations. The accuracy and sensitivity have been determined by measuring the time-of-flight of light at extremely low levels of light intensity. These results show that the instrument is capable of a wide variety of measurements.

Applications of Radiative Lifetime Measurements

Measurement of radiative lifetimes provides data for many theoretical and applied problems. These include quantitative analysis by spectroscopy, kinetics of energy transfer and degradation, and knowledge of the electronic structure of atoms and molecules.

One of the main purposes of this laboratory in developing this technique is application to high-temperature systems. One such is the accurate determination of thermochemical data for gas-phase species. Measurement

of the rate of emission of radiation permits calculation of the rate of absorption (See Part II of this report). This is in turn used to infer the number of molecules that are absorbing radiation in an equilibrium situation, hence solid-vapor equilibrium constants. These equilibrium constants plus entropies from the accurately known spectroscopic data permit much more accurate determination of thermodynamic data than hitherto possible.[1] Other intriguing possibilities are the use of the absorption coefficients to determine absolute quantities of molecules in the reversing layers of stars, in flames, and in rocket exhausts.

Very little is known about absolute rates of energy transfer. The radiative lifetime of iodine has been used in Part II to convert to absolute values the extensive determinations of relative values of cross sections for vibrational energy transfer by collision. Future utilization of solar energy will depend on the ratio of nonradiative to radiative decay in the energy-conversion medium. In fact, extensive measurements already are being carried out on systems important in photosynthesis, where the lifetimes of radiation are in the microsecond to millisecond range. On the other hand, scintillators depend on the extremely short radiative lifetimes for maximum efficiency, and one chooses scintillators that give efficient reconversion to radiative energy.

Information on the electronic structure of matter can be inferred from lifetime measurements, since transition probabilities depend on the wave functions. Experimental data could be used to check calculations of absolute transition probabilities based on assumed wave functions. Sum rules for radiative transition probabilities should be checked by measuring the lifetimes of different bands in a given system as is possible in the iodine molecule, for example. The nature of color centers in

crystals, and of conductors in semiconductors can be inferred from measurements of lifetime as a function of impurities present. In fact, any one of these experiments makes building a lifetime apparatus very desirable.

Instrumental Requirements

It is possible to specify certain instrumental requirements set by the systems to be studied. Once known, these can be met by alteration of various parts of either the optical or electronic systems of the total apparatus, whichever is more convenient. These key quantities are the lifetime to be measured and the photon flux that constitutes the signal.

Range of Lifetime.

Lifetimes of interest range between 10^{-5} and 10^{-9} sec. Equation (A - 1),

$$\lambda = 1.51\ \lambda^2\ (g_2/g_1)\ (1/f)\ , \qquad (A - 1)$$

gives the shortest lifetime for visible light as about 10^{-9} sec, since both the oscillator strength, f, and the ratio of statistical weights (g_1/g_2) are about unity, and the wavelength is about 4×10^{-5} cm. It should be noted that if this time is to be known within 1%, then the path length traveled by the fluorescent light must be constant within 0.3 cm because the velocity of light is finite. The longest lifetime of interest is set empirically by the fact that the transition must be strong (value of oscillator strength, f, near unity) in order for it to be observed, and in order for the lifetime to be unaffected by collisions and other perturbations. A usable criterion is that the oscillator strength be greater than 10^{-4}, resulting in a longest lifetime of about 10^{-5} sec.

The relation between lifetime and observed phase shift is given by Eq. (A - 2) (Cf. Section C, Theoretical),

$$\tan \phi = 2\pi ft, \qquad (A - 2)$$

where ϕ is the phase shift, f is now the frequency of modulation, and t is the lifetime. For best use of the instrument, one would like tan ϕ to equal unity. With frequencies such that tan ϕ is not equal to 1, the phase angle must be known more accurately for a given precision in lifetime. Furthermore, as $2\pi ft$ becomes much greater than unity, the signal level decreases, since the decay is exponential and results in a decrease in the modulation of the fluorescent light. Thus, one should choose a modulation frequency such that $2\pi ft = 1$. If not, accuracy and effective sensitivity are sacrificed.

Signal Levels.

The amount of signal energy available from molecules with discrete spectra in the gas phase is extremely small, and on the order of 10^4 or more smaller than that available from fluorescent material in solution. Consider that we have a source of exciting light of given brightness temperature (or energy output per wavelength interval). Then, the fluorescent energy must be proportional to this energy output times the amount absorbed. The maximum absorption permissible is about 10%, because larger absorption results in multiple absorption and reemission which leads to a measurement of a diffusion rate rather than a lifetime. The width of the absorption is determined by the Doppler widths of the gas-phase systems and is on the order of tenths or hundredths of angstroms. In favorable cases, band systems or heads may be used, and the absorption will be multiplied by approximately the number of lines present. Since

the energy available is proportional to the area under the absorption curve, and since solutions have smeared out absorptions tens or hundreds of angstroms wide, signal levels for the gas phase are lower by factors up to 10^4.

In addition, the absolute amount of fluorescent energy available is determined further by the optical "speed" of the light-modulating apparatus; by the attenuation of exciting and fluorescent light by color filters; and by apparent attenuation of fluorescence yield by transitions to which the photomultiplier is not sensitive.

The experimental situation, while difficult, is best when excitation is at a band head or region of great line density, when the light sources are extremely bright, and when the optics have a large aperture. Excitation over a complete band head is difficult because few light sources of the proper specifications are available. At present, the brightest light sources available seem to have about 5,000°K brightness temperature,[2] and the largest usable area of source is set by the admittance aperture of the supersonic grating at 1 mm x 25 mm. The fastest optics feasible are between f 1 and f 5, depending on the quality of the lenses and the need for a monochromator for the exciting light.

Even when all of these factors are optimized, the signal level is extremely low, and rather elaborate electronic techniques for handling the signal are necessary. The instrument that will be described has been tested and shown capable of measuring these short times even with the small signals available.

Review of Methods for Measuring Radiative Lifetimes

Although measurement of radiative lifetimes by direct and indirect methods has a history of more than thirty years, there seems to be no complete classification or review of the various methods. In view of the great activity and interest in lifetime measurements, such a review is in order. The main purpose of this review is to provide a framework for keeping track of current publications, as well as a background for evaluating the present apparatus. It will, therefore, indicate the methods, give references to characteristic papers; and, in the case of similar techniques, indicate other important papers and groups of workers.

Reviews of methods, as well as of theory and of data, are given by Förster,[3] Mitchell and Zemansky,[4] and by Pringsheim.[5] Techniques reviewed by these authors will be given only brief mention here.

Classification is according to salient experimental features. The main division is between methods that require knowledge of the number of molecules or atoms present, and those which do not. For the most part, the first group involves measurement of steady-state or equilibrium emission or absorption intensities. The second group involves mostly, direct measurement of decay lifetimes. The latter group includes those methods that are essentially similar to the Becquerel phosphoroscope common to biological laboratories; those that yield a time-resolved plot of fluorescent intensity, similar to the radioactive-decay curves; and those methods, such as the present one, that measure the phase shift of a modulated light beam produced by the finite time it takes the molecule to absorb and re-emit light.

Methods that Require Knowledge of the Number of Molecules

The first method is measurement of the absolute absorption coefficient, or Einstein B coefficient, plus, in some cases, the relative intensities of fluorescences from the given upper state. This method is fully discussed elsewhere with the measurements made on the iodine molecule. Conversely, one can measure absolute emission intensities and, if the upper-level population is known, calculate the first order decay constant, or Einstein **A** coefficient.

Another method involves measuring the magneto-rotation at the edges of an atomic line originating in a populated level. Plane-polarized, monochromatic light is passed longitudinally through a gas sample placed between the poles of a magnet. The amount of rotation is a simple function of the number of molecules, oscillator strength (f), magnetic field, and separation between the frequency of the absorption line and that of the light used.

The index of refraction of a gas changes rapidly at the edges of a line, and the resulting anomalous dispersion may be measured interferometrically by the Roschedestwensky "hook method." This method has yielded some of the best f values for atomic lines yet obtained and is currently being used very widely in Russia.[6] A Jamin interferometer is crossed with a stigmatic spectrograph, producing a set of hook-shaped fringes. The spacing of these fringes is simply related to the f value, the wavelength, and the number of absorbing atoms.

Another method, suitable for atoms with lifetimes less than 10^{-7} sec is the measurement of magnetic depolarization. If excitation is by polarized light, the fluorescence also will be polarized. However, if the excited atoms are caused to precess at a known rate by a magnetic

field, the fluorescence will be depolarized. Measurements of depolarization as a function of field strength can then be related to the time spent in the excited state. This method is best for lifetimes shorter than 10^{-7} sec. Rotational depolarization may be measured for large molecules with short lifetimes ($< 10^{-9}$ sec). This is particularly effective in solutions.

A variant of the absolute-absorption experiment which avoids the necessity for exact vapor-pressure data is absolute absorption by a molecular beam as developed by Kopferman and Wessel,[7] and by King and co-workers.[8] The density of molecules in the absorbing section of a molecular beam is measured directly at the time of experiment by weighing the efflux of the beam. The technique is quite difficult, but seems to have given fine results. So far, it has been applied only to atomic species, but it could be applied readily to molecular species if the vapor-phase composition were known and if the spectra were simple enough.

Relative emission intensities of a number of atomic species in an arc between electrodes of known composition were measured by Allen and Asaad.[9] Oscillator strengths were calculated on the assumption that the gas-phase composition was the same as that of the solid electrode.

Methods that Measure Time Directly and Are Independent of Knowledge of Concentration

The phosphoroscope was first described by Becquerel in 1867.[10] It consists essentially of two gates or shutters that may be made to open periodically for a known period of time and staggered from one another by a given "phase difference." The first gate admits the exciting energy, the second permits observation of the fluorescence after a specified time.

The earliest devices, which are still widely used for times longer than a millisecond, employ mechanical shutters. An example of this type of shutter is two slotted discs rotating on the same axis, the slots of one disc being out of phase with those of the other. The intensity of fluorescence is measured as a function of the phase difference of the slots and the speed of revolution. Interpretation of these results is somewhat complicated, and Pringsheim should be consulted for references.[5] Instruments intended for times as short as millimicroseconds employ also inertialess shutters such as Kerr cells,[11] supersonic gratings, or grids that pulse an electron beam that provides excitation energy.[4] High-speed phosphoroscopes, or fluorometers using Kerr cells were designed by Gaviola[12] and by Szymanowski,[13] while Maercks[14] describes one using a supersonic grating. In all three of these instruments, the phase difference between the two shutters is varied by changing the length of the light path over a range of 10 meters. Using a Kerr cell to pulse his exciting light and a photocell operated on pulsed direct current, Ziock measured output current of the photocell as a function of the time interval between the pulse of exciting light and the pulse sensitizing the photocell.[15] These results were then compared with theoretical curves for various lifetimes.

An extremely active group in the use of phosphoroscopes ("taumeter," "ultrataumeter") is that of Tolstoi.[16] These workers have designed unique mechanical shutters and electronic equipment that they have used between 10^{-3} and 10^{-7} sec. Their work covers a very wide field of application and appears to be quite careful.

Time resolution methods involve populating some excited level with a pulse of energy and observing the fluorescent intensity as a

function of time. The resulting decay curve is similar to those for nuclear decay. The main difficulties for millimicrosecond lifetimes are obtaining a sufficiently well defined or square pulse of exciting energy, for which light and electrons have been used, and determining an accurate time scale.

Earliest workers used the thermal velocity of gas molecules to obtain time resolution since neither displacement of the fluorescence in a vapor jet nor broadening of a sharply defined fluorescence beam by Brownian motion is observed with iodine, the lifetime must be longer than 10^{-6} sec. A sophistication of this technique is to determine fluorescence intensity in a molecular beam as a function of distance from the exciting light beam. This method is severely limited, as molecular speeds are on the order of 10^4 or 10^5 cm/sec. However, in some instances, it is possible to expand the time scale by using either rapidly moving canal rays or molecules that were accelerated as ions and underwent charge transfer.

Alternatively, one can pulse the light source electronically and obtain time resolution by using fast recorders or oscilloscopes. Calvin and his co-workers describe a system that uses a flash tube for excitation and both oscilloscopes and mechanical recorders in parallel to measure, simultaneously, decay times ranging from milliseconds to seconds.[17,18] A specially developed hydrogen flash tube with a millimicrosecond decay time in conjunction with an oscilloscope as time resolver was used by Brody to measure millimicrosecond-lifetime solution fluorescence.[19] Accuracy of 30% is obtained. Whetstone describes another pulsed light source that might be useful for this type of measurement.[20]

In order to avoid the necessity of obtaining special pulsed light sources, other workers have used well-defined pulses of electrons to supply excitation-energy. This method has the difficulty that highly energetic electrons are needed in order to make their transit time less than the time to be measured. Such energetic electrons can cause dissociation or ionization, as well as excitation to levels higher than that of interest so that one observes an intermediate stage of a cascade process. However, Heron, McWhirter, and Rhoderick used this method successfully to measure lifetimes of excited helium on the order of 10^{-7} sec.[21] Bennett and Dalby also have used electron excitation plus a variable-delay pulsed photomultiplier for time resolution to measure the first negative bands of N_2^+.[22] They seem to have corrected for the effects of cascade processes and of overlap bands. Lifetimes measured are on the order of 10^{-7} sec. Wertheim and Augustyniak have used pulsed electrons from a Van de Graaff generator to excite carriers in semiconductors; lifetimes from 10^{-5} to 10^{-8} sec have been measured.[23]

An alternative method of obtaining both time resolution and/or square light pulses is that of rapidly rotating mirrors. Clades, Jones, and Wickersheim have described a high-speed light-pulse shaper.[24] High-speed rotating mirrors are used also for mega-frame-per-second cameras and for time-resolution work. Beams has described methods of suspension, etc.[25] Tsui has described a system for time-resolved spectra using a rotating mirror and spark discharge.[26] Phillips has proposed a very interesting lifetime apparatus using rotating mirrors.[27] The exciting light is reflected from the rotating mirror and swept across the container of sample. The fluorescent light is then reflected from the same mirror face which sweeps it along the slit of a stigmatic spectrograph. The

unique feature of his arrangement is that the position at which the fluorescent light from any given volume element of sample strikes the slit (hence the position on the plate) depends only on the time after the passage of the beam of exciting light through that volume element. It is independent of position in the sample cell. The wavelength dispersion permits investigation of many features simultaneously, while the photographic recording permits integration of light intensity over long periods of time.

The last method to be discussed, and the one that seems to be most widely used at present is the phase-shift method. A difference between the phase occurs because the atom or molecule holds the energy for a finite period of time before reemitting it. The relation between phase shift and lifetime, τ, is obtained by expanding the amplitude modulation as a Fourier series and by assuming a first-order decay law for fluorescence (see Section C, Theoretical). The result is, as one might expect:

$$\tan \phi = 2\pi f \tau ,$$

where ϕ is the phase shift for, and f the frequency of a given Fourier component. In practice one uses only the fundamental, which we shall call the first harmonic.

Phase-shift methods may be classified further according to the method of producing modulation. A mechanical method for producing modulation in the 10^5- sec^{-1} range utilizing a rotating reflection grating has been built by Brewer and co-workers.[28] A Kerr cell modulator (see also under phosphoroscope method) for studying photoconduction is described by Harnik, Many and Grover.[29] The most widely used modulator is the supersonic grating which has the advantage of wide spectral range and other mechanical advantages. (See also the description of optical components of

this apparatus, Section B.) This has been developed extensively in Hanle's laboratory,[14,30] most recently by Schmillen, for use on solutions and crystals. At Berkeley, Rollefson and Gwinn and co-workers designed equipment for solution work,[31,32] while our group is developing the method for gas-phase application. In Russia, Tumerman was one of the pioneers in using this method.[33] Bonch-Bruevich and co-workers have been quite active on solution measurements and appear to have done quite careful work using and analyzing the method and its applications.[34-36] Venetta has designed a modification of the Rollefson apparatus for study of biological fluorochromes under a microscope.[37]

B. DESCRIPTION OF THE APPARATUS

The apparatus is modeled after that designed by Bailey and Rollefson,[31] and by Kroman[32] for solution work, and has been modified and redesigned to make it suitable for measuring signals from gas-phase systems. Work on the gas-phase apparatus was started by C. Geoffrey James and Kenneth Lamers at the University of California and continued by R. G. Brewer.[28] The electronic portion of the equipment reported on here and described in detail in the Appendix is a result of major modification of Brewer's apparatus by Jerry M. Sakai of the Lawrence Radiation Laboratory Electrical Engineering group and the author. While in over-all principle the apparatus is unchanged, almost all of the details of the electronics and the physical design as well as the principles of the frequency control mechanism and the phase detector are different. These changes have greatly reduced extraneous noise and have permitted the measurement of the time of flight of light to be described in Section C. This measurement constitutes a significant trial of the apparatus because of the low light levels used.

The general scheme of the apparatus is shown in the block diagram, Fig. 1. Light from the source passes through a supersonic-grating modulator which modulates at 5.205 Mc. Part of the light is reflected by a scatterer (barium sulfate suspension chosen for its stability[38]) into the "reference" channel photomultiplier. The remainder passes through either a cell containing the sample or one containing a $BaSO_4$ suspension. A phase difference between the outputs of the reference and sample channels is observed both with fluorescent material and with sol in front of the sample photomultiplier. The difference of phase differences is due to

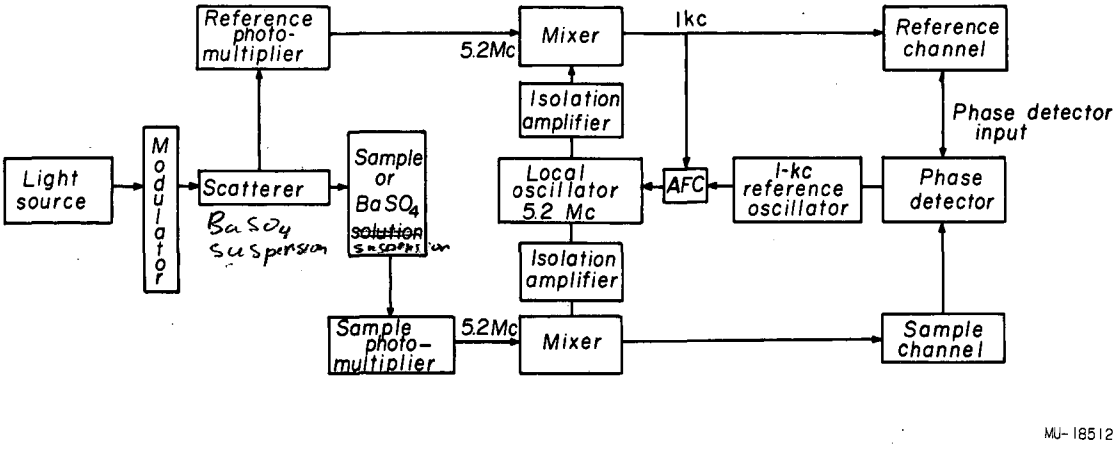

Fig. 1. Block diagram of millimicrosecond lifetime apparatus. (For details, see Lawrence Radiation Laboratory engineering drawing No. 4V9201).

the finite lifetime of the fluorescent material and is measured by the use of the calibrated phase shifters plus the null-indicating phase detector.

Optical Equipment

The optical part of this equipment consists of a high-intensity, monochromatic light source, an amplitude modulator, sample containers, and light detectors.

Light Sources

Light sources for this apparatus must have very special characteristics. Their brightness temperature or intensity at the wavelength of interest must be extremely bright in order to provide an adequate signal and signal-to-noise ratio at the photomultiplier. Furthermore, they must supply energy only at the wavelength of absorption of the sample molecule because of the problem of scattered exciting radiation. For instance, if the exciting line were ten times as wide as the absorption, then scattering of only 1% would give a component as large as the fluorescence. This problem is ameliorated by observing only fluorescence of a different wavelength than the excitation, and by using discrete line sources. This also precludes the need for achromatic optics. For the present tests, an A100-H4 mercury arc was used with Wratten 77A and didymium glass filters to pass only the green line. The problem of light sources is discussed by Worden.[3]

Modulator.

Light modulation is by the method described by Brewer,[28] by Bailey and Rollefson,[31] and by Kroman.[32] The essential details are shown in Fig. 2. The light source, H, is imaged on the first slit, S_1, which then acts as an effective source. Light from S_1 is rendered parallel by lens

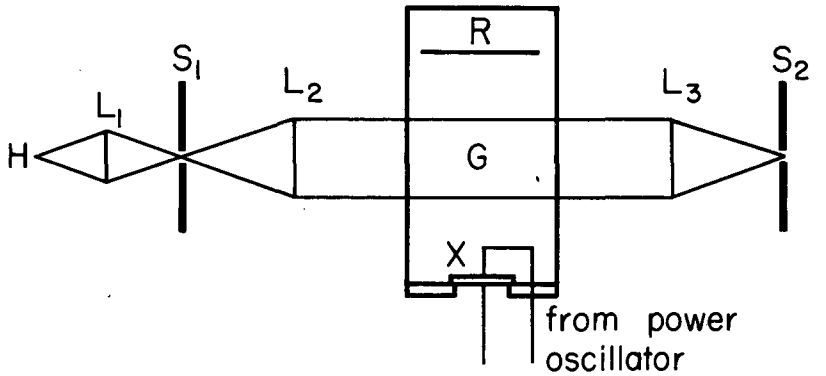

H	*A-H4 Mercury light source*
L_1	*Glass lens, 10 cm focal length, 5 cm diameter*
L_2, L_3	*Glass lenses, 20 cm focal length, 11 cm diam.*
S_1, S_2	*Slits*
X	*X-cut quartz crystal*
R	*Stainless steel reflector*
G	*Ultrasonic standing wave*

MU-15661

Fig. 2. Light modulating unit--schematic.

L_2, passes through the supersonic grating G, and is focused by lens L_3 on the second slit. When the refractive index is uniform across the supersonic grating, all of the light is focused on S_2. A piezoelectric crystal, X, sets up a standing wave G, in the water tank, and as the rarifications and condensations form, the water acts as an intermittent grating. Light is thrown into a diffraction pattern on either side of the slit, causing a decrease in the intensity transmitted through S_2 and the light issuing from S_2 is modulated. Since the grating forms and collapses at twice the frequency of the oscillator driving the quartz transducer, X, the frequency of modulation is twice the oscillator frequency.

There are many papers on the supersonic grating and its applications. A number of these are listed here, and although they do not all deal with modulation or with lifetimes, they do contain information on producing the supersonic grating and on associated phenomena. The grating effect was described first by Debye and Sears[39] and by Lucas and Biquard.[40] Much work was then devoted to looking for a charge-separation (Debye) effect in salt solutions.[39-51] Bär studied the coherence of light diffracted by the grating and found that the frequency of the light in diffraction order n was changed by n times the modulating frequency.[52] His work was confirmed theoretically by Raman and Nagendra Nath who analyzed the effect of standing and traveling waves perpendicular to transmitted light.[53] Their result for the angle of diffraction caused by the standing wave is the usual grating equation: $\sin \beta = - n\lambda/\lambda^*$, where β is the angle of diffraction of the light in order n, and λ and λ^* are the wavelengths of the light and of the supersonic wave. The shift in frequency, f, is given by $f = f^0 \pm nf^*$.

Cady gives a review and list of references on crystal transducers,[54] while Brown and Frankel suggest an improved transducer mount.[55] References mentioned in Section A should be consulted for applications of supersonic gratings to the lifetime problem.

Sixty-kilocycle Modulator.

In addition to the supersonic grating modulator, a 60-kc rotating reflection-grating modulator is being readied for use and will be incorporated into the present electronic equipment by modifying only the automatic frequency control and the frequency reduction units.[28]

Evaluation of Modulator.

Recent experience with the supersonic grating modulator indicates that the criterion for choosing between different types of modulators might be reconsidered and reapplied. Succinctly, the best modulator for the lifetime apparatus is that which provides the largest signal-to-noise ratio at the input to the electronic system. The specification of "signal-to-noise ratio" rather than "signal" should be stressed since the discussion of instrumental sensibility will show that the signal-to-noise ratio rather than the amplification of the system limits the sensibility of the apparatus. This criterion may be resolved into three components -- the spectral range, the optical aperture, and the efficiency of modulation.

The spectral range of the modulator is limited by the material of construction of the lens, window, and supersonic grating. This range is limited to the ultraviolet by the opacity of quartz and air at 2000 A and to the red by the insensitivity of photomultipliers beyond $\sim$ 6000 A. The present modulator uses water, while others have used such materials as toluene[14] and xylol.[35]

By optical aperture is meant the largest size source usable and the aperture of the lens system. The largest size source so far used is 1 mm x 25 mm and is limited by overlap between orders of the diffraction pattern at slit 2. The optical speed has been limited by the quality of the lenses and difficulties in alignment to f 12, but might be increased to f 4. Using the numbers of Brewer,[28] who used f 3 optics, the fraction of light emitted by the source that is passed by f 4 optics and reaches the sample container is 3×10^{-4}. The actual signal reaching the photomultiplier is smaller still by the fraction of modulation and the efficiency of collection of fluorescent light.

The fractional modulation of the light is a quantity that has not been given sufficient attention. We will define quantities of interest, relate them to experimentally observed quantities, and then criticize that relation.

Not all of the modulated light reaches the sample cell, because of geometrical limitations, and therefore the total amount of modulated light is used to judge the efficiency of the modulator. Only that part of the light which reaches the sample cell is used to estimate the signal-to-noise ratio by Eq. (C-12).

The fraction of energy modulated has been related to experimental quantities in the following way.[31] Assume that the light is modulated only at 5.2 Mc (first harmonic). Then the light passed by slit 2 will consist of a dc component and a 5.2-Mc component. The fraction of light passing through slit 2 that is modulated is the energy in the 5.2-Mc component divided by the total energy (dc + 5.2 Mc). Since modulation is produced by periodic attenuation of the beam of light, and since,

under the assumption of only first-harmonic modulation, the energy removed is exactly equal to the energy in the 5.2-Mc component, the following relation holds:

$$\text{fraction modulated} = \frac{I^0 - I}{I} = \frac{\text{energy in 5.2-Mc component}}{\text{total energy in beam}} . \qquad \text{(B-1a)}$$

The fraction of energy transmitted with the modulator off is

$$\text{fraction}' = \frac{I^0 - I}{I^0} = \frac{\text{energy in 5.2-Mc component}}{\text{energy transmitted with modulator off}} , \qquad \text{(B-1b)}$$

where I^0 is the energy measured with, for example, the modulator off and using a phototube with a long time constant, and I is the total energy with the modulator on.

Equation (B-1a) has been used to evaluate the performance of the modulator. However two observations cause suspicion on its validity. First is the observation of spurious phase shift due to changing the position of the reflector, R, which is discussed later. Second is the reproducible observation of fraction modulation greater than unity. The assumption that all of the modulation is first-harmonic is suspect and should be verified experimentally. It certainly may be very poor if the quartz transducer, X, is being driven too hard. Similarly, the opacity of the supersonic-grating medium may be increased by application of the driving voltage. Seemingly unrealistic, but possible causes of such an increase are stirring up of "dust" in the water, or formation of tiny bubbles due to cavitation. Finally, the presence of standing or traveling waves, chronologically out of phase with one another, has been observed and is discussed in more detail later. If such standing waves are always present somewhere in the tank along the path of the light

beam, that is, the density of the grating medium never is completely uniform, Eq. (B-1a) could very readily give fractional modulation greater than unity.

Spurious Phase Shifts.

In the earlier measurements with this apparatus, we came across a phenomenon that could limit severely the accuracy of the method. By the use of a mirror to divert the lower half of the modulated light beam into the "reference" photomultiplier and a scatterer to divert part of the remainder into the "sample" photomultiplier, phase shifts up to 180° were observed on changing the position of the reflector, R, (Fig. 2) in the supersonic-grating water tank. Close examination of the image of Slit 1 as the reflector position was varied showed diffraction patterns first only at the top, then the center, and then perhaps the bottom of the slit. Examination of the image of the grating itself showed that both standing and traveling waves could be set up in different parts of the tank depending on the position and orientation of the reflector. Alignment of the water tank and of the reflector to produce any diffraction pattern at all is difficult and precise and no further alignment would eliminate the spurious diffractions on different parts of the slit image.

A pinhole orifice mounted on a rack and pinion was used to investigate this effect further. First the pinhole was set at the center of the diffraction pattern and the photomultiplier was moved behind the orifice. The phase shifts produced with this setup were measured and were no more than 5° using a 10-stage 6655 photomultiplier with total applied voltage of 900 v. This gives an upper limit to phase shifts caused by differences in transit time for electrons from different parts of the photocathode.

Next, the pinhole orifice was scanned either horizontally or vertically across the image. This produced continuous phase variation over a range of 180°. At this time the water tank and optics were in such good alignment that a broad and sharp diffraction pattern was obtained with a narrow slit. Even with slits 1 mm wide, 65% modulation was obtained, which tends to lower the effectiveness of the modulator. Furthermore, the entire inside of the tank, except for the quartz-crystal transducer and the reflector plate, was lined with Styrofoam to deaden reflections of the sound waves, and lens L_2 was stopped down to about 1/4 in. wide by 1/2 in. high.

This spurious phase shift was eliminated completely by making sure that the light reaching each photomultiplier is sampled from over exactly the same areas of the modulated light beam. This is accomplished by the use of a low optical density ($\sim$ 10%) $BaSO_4$ suspension to scatter light into the reference photomultiplier and by stopping down the light beam so that all of the cross section going through the "reference" scatterer enters the "sample" container and is observed by the "sample" photomultiplier.

Spurious phase shift due to the chromaticity of the optics and the modulator is unlikely if only one wavelength is used during a complete measurement. The phase difference with scatterer in front of the "sample" photomultiplier should be measured using light of the exciting wavelength.

This supersonic grating modulator is extremely sensitive to both physical vibrations and alignment of the optics. Modulation of 65%, measured according to Eq. (B-1) was obtained with 1-mm-wide slits and f 10 optics. Using the same slits and f 20 optics (lens 1 was masked down further), 100% modulation was obtained.

The question of modulation by the supersonic grating recently has been studied in some detail by Bonch-Bruevich and Molchanov.[35] They too have observed different phases of modulation from different parts of the modulator and report amelioration of the observed phase uncertainty by sampling for "reference" and "sample" photomultipliers from exactly the same sections of the modulated beam. However, they do not indicate their means of sampling. Phase stability of 0.4° is reported over a 15-min. period; however this might be improved, since their apparatus has no provision for adjusting the orientation of the reflector plate, R, in the water tank. These authors point out also that this dispersion of phase over position makes the effective modulation less than that measured by the technique indicated by Eq. (B-1b). Their grating material is xylol, not water as used in our apparatus.

Light Detectors

The light detectors used were RCA 6655 photomultiplier tubes. These have S 11 response and current gain of about 10^6. They are being replaced by 7264 tubes that have the same photocathode but 10^2 greater current gain and much smaller dispersion of photoelectron transit time (rise time).* The importance of the small dispersion of transit time is evident; that of the higher gain is that it either reduces the burden on the successive vacuum-tube amplifiers or permits operation with less dark current.

---

*The author is indebted to Mr. R. A. Berg for obtaining these tubes and the associated circuitry.

Electronics

The important components of the electronic system are shown in the block diagram (Fig. 1). The output of the photomultipliers observing the reference scatterer and the fluorescent material are fed into two distinct and physically separate channels called the "reference" and the "sample" channels which are identical except for a radio-frequency amplifier preceding the mixer in the "sample" channel.

Frequency Conversion

The 5.2-Mc signal from the photomultipliers is converted to 1 kc without loss of phase information. This is done for several reasons. First, at 1 kc there is less chance of picking up stray signals from the air and of coupling between the channels. Then, since large-value components must be used, stray capacitances in the calibrated phase shifters are not important. Finally, narrow-band width filters (e.g. 4 cps bandwidth) are readily made for the low frequency, and the 1-kc beat signal may be held within very close limits. The last two points are significant because the random noise content of the signal is proportional to the inverse square root of bandwith, and because phase uncertainty in a narrow band-pass filter caused by frequency uncertainty is proportional to the absolute value of frequency uncertainty divided by bandwith (Eq. (C-13)).

Automatic Frequency Control

Accurate control of the 1-kc beat frequency is obtained with a servo mechanism called the "automatic frequency control" (AFC). In this servo, the frequency standard, which determines the accuracy and stability, is the oscillator controlled by a tuning fork to $\pm$ 0.1 cps. The sensing element of the loop is a phase detector, which produces

an "error" signal proportional to the cosine of the phase difference between the standard and the reference-channel signal. As the reference-channel frequency starts to change, the phase difference also changes, changing the "error signal" which drives the control element, a variable capacitance diode in the tank circuit of the beat oscillator.

Since the error signal is produced by a phase difference, there is no steady-state error in the beat frequency which tracks exactly the "standard" and therefore is constant to $\pm$ 0.1 cps. Transient errors are reduced by the amount of the loop gain, a factor of 100.

Calibrated Phase Shifter

In both the sample and reference channels, the frequency-controlled 1-kc signal is amplified and fed into calibrated phase shifters. It is the setting of these components that ultimately is related to lifetime. The values of the components producing the phase shifts are known to 1 part in 10^4, which is also the limit set by their variation with temperature.

Phase Detector

The final element, common to both channels, is a long time constant phase detector used as a null meter. It is this component that limits the sensibility of the instrument.* With clean (signal-to-noise ratio of 15 to 1) input, the sensibility for a single reading is 0.2°. With practical signals, the sensibility decreases and will be discussed later. Since this phase detector is used as a null meter, it is essentially independent of input-signal amplitude. Its long time constant of $\sim$ 1 sec tends to average out random noise.

---

*We draw the important distinction between sensitivity, which is given in units of, say, degrees per scale division, and sensibility which is the smallest increment that the instrument can sense.

C. EVALUATION OF THE APPARATUS

Lifetime is related to phase shift by the solution of a differential equation giving $\tan \phi = \omega \tau$. Uncertainty of the knowledge of τ depends on the value of $\omega\tau$ and on the uncertainty in measuring the phase angle, ϕ. At present, the limiting uncertainty in measurement of ϕ occurs in identifying the null point at the phase detector and is caused by the noise components of the "sample" channel signal; the noise components may be reduced by narrow band-pass electronic filters, in which case phase knowledge eventually becomes limited by uncertainties in phase caused by fluctuations of frequency. However even with the wide-band system used here and with light levels corresponding to those of fluorescence from, for example, iodine, the phase may be identified within 0.5°. This means that lifetimes between 6.4×10^{-9} and 10^{-7} sec may be measured with less than 20% uncertainty.

The accuracy of the instrument can vary greatly from run to run because of possible systematic errors. However measurement of the speed of light with extremely low light levels indicates that the intrinsic instrumental accuracy is within the limits of sensibility.

Theoretical Considerations

Relation of Phase Shift to Lifetime

The differential equation relating the time-dependent modulation of fluorescence to any arbitrary, periodic modulation of the exciting light and to the radiative lifetime has been solved by Bailey and Rollefson.[31] The general result is

$$I(t) = \frac{a_o}{2}\frac{k_2}{k_1} + k_2 \sum_n \frac{a_n \sin(n\omega t - \phi_n)}{[k_1^2 + (n\omega)^2]^{1/2}} \quad . \qquad (C\text{-}1)$$

Since the apparatus is tuned only to the first harmonic,* Eq. (C-1) reduces to

$$I(t) = \frac{a_o}{2}\frac{k_2}{k_1} + \frac{k_2}{(k_1^2 + \omega^2)^{1/2}} a_1 \sin(\omega t - \phi) \quad . \qquad (C\text{-}2)$$

In these equations k_1 is the sum of all depopulation rate constants, radiative and nonradiative, and equals $1/\tau$, the reciprocal lifetime; k_2 is proportional to the amount of absorption of exciting light; ω is 2π times the frequency of modulation; the a's are the Fourier coefficients describing the exciting light; and ϕ is the phase angle, which is related to lifetime by

$$\phi = \tan^{-1} \omega \tau \qquad (C\text{-}3)$$

---

*Higher harmonics are rejected electronically, but still might be troublesome if present because all light striking the photomultiplier contributes to the shot noise.

Relation of Fraction of Modulation of Fluorescent Light to Lifetime

It is interesting to note that the fraction of the fluorescent light that is modulated depends both on the fraction of the exciting light modulated and on the lifetime. The fraction of the exciting light modulated is $2a_1/a_0$ [cf. footnote in discussion of modulator, Part B, Eq. (B-1)], where $a_0/2$ and a_1 are the amplitudes of the dc and first harmonic terms in the Fourier series. From Eq. (C-2) the fraction of fluorescent light modulated is

$$\text{fraction modulated} = \frac{2a_1}{a_0} \frac{k_1}{(k_1^2 + \omega^2)^{1/2}} = \frac{2a_1}{a_0} \frac{1}{(1 + \omega^2\tau^2)^{1/2}} . \qquad (C\text{-}4)$$

Instrumental Sensibility

Relation of Uncertainty in Lifetime to Uncertainty in Phase Angle

Eq. (C-3) may be used to give the relation between uncertainty in the measured phase angle and the uncertainty in lifetime. By differentiating Eq. (C-3) and rearranging, we have

$$\frac{\Delta \tau}{\tau} = \frac{(1 + \omega^2 \tau^2)\, \Delta \phi}{\omega \tau} , \qquad (C\text{-}5)$$

where a term $\tau \Delta \omega$ has been dropped. A useful form of Eq. (C-5) is a plot of $\frac{\Delta \tau}{\tau}$ as a function of $\omega \tau$ with a $\Delta \phi$ as a parameter. The minimum is $(\Delta\tau/\tau) = 4 \Delta \phi$ for $\omega \tau = 1$.

Solving Eq. (C-5) for the upper and lower limits of τ, $\tau_{1,2}$ for given values of $\frac{\Delta \tau}{\tau}$ and of $\Delta \phi$, we have

$$\omega \tau_{1,2} = \left(\frac{\Delta \tau}{\tau}\right)\left(\frac{1}{2 \Delta \phi}\right) \left[1 \pm \sqrt{1 - 4\left(\frac{\Delta \phi}{\Delta\tau/\tau}\right)^2} \right] . \qquad (C\text{-}6)$$

In using (C-5) and (C-6) it should be borne in mind that $\Delta \phi$ might vary with τ. One such cause is the variation of modulation of fluorescence with lifetime indicated by Eq. (C-4). According to the discussion of Instrumental Sensibility which follows, $\Delta \phi$ may be taken as equal to $\sqrt{2}\, \Delta \xi$, where $\Delta \xi$ is the uncertainty in identifying the null at the phase detector.

Phase Sensibility

Phase Sensibility of the Key Components. There are three angles that are of interest in a determination of lifetime. Of these, two are those measured by the calibrated phase shifter and by the phase detector, either of which may limit the sensibility of the instrument.

Quantitative discussion requires precise definition of the three angles. The first is related to the lifetime by Eq. (C-3),

$$\phi = \tan^{-1} \omega \tau \,, \qquad \text{(C-3)}$$

where ω is the modulating frequency in radians/sec. The second angle is the phase shift caused by the calibrated phase shifter

$$(\Theta C/2) = \tan^{-1} \omega' \, C \, R_i \,, \qquad \text{(C-7)}$$

where ω' is the beat frequency, $2\pi kc$; C is the capacitance; and R_i is the resistance at null with either fluorescent material or sol in front of the "sample" photomultiplier. The angles ϕ and Θ are related by

$$\phi = \left| \Theta_{\text{fluorescent material}} - \Theta_{\text{sol}} \right| . \qquad \text{(C-8)}$$

The third angle is the phase difference between the "reference" and "sample" signals at the phase detector and is denoted by ξ. The angle ξ is 90° at the time of a reading, producing a null indication from the phase detector since the output is proportional to $\cos \xi$.

The sensibility of the instrument may be limited either by the determination of the angle $(\theta/2)$ in reading the phase-shifter settings, or by the determination of the null point at the phase detector with angle ξ equal to 90°.

Sensibility of the calibrated phase shifter. The precision of the phase shifter is obtained from Eqs. (C-9) and (C-10):

$$\frac{d \tan \theta}{\tan \theta} = \frac{d \omega}{\omega} + \frac{d R}{R} + \frac{d C}{C} . \qquad (C\text{-}9)$$

The frequency (1000 cps) is known to 0.1%; resistance to 0.1%, and capacitance, including stray capacitance, to 0.1%. Therefore, tan θ is known to a few parts in 10^3. Equation (C-10) relates $d\theta$ to d tan θ.

$$d\theta/\theta = \cos^2 \theta \ (d \tan \theta/\tan \theta) . \qquad (C\text{-}10).$$

It is seen that to a good approximation, the uncertainty in θ is the same as in tan θ or 0.2%.

Sensibility of the phase detector. The uncertainty of measurement at the phase detector, $\Delta \xi$, may be resolved into three components:

$$\Delta \xi = \Delta \xi_o + \Delta \xi_{noise} + \Delta \xi_{frequency} . \qquad (C\text{-}11)$$

The first component, $\Delta \xi_o$, is that for clean and stable signals. The second component is due to noise in the signal reaching the phase detector. The third is due to phase shifts in tuned circuits caused by shifts in frequency. These components will be discussed in the next section.

Discussion of limitations on instrumental phase sensibility. The sensibility of the phase detector is 0.2° and is much larger than that of the calibrated phase shifters. Therefore, the instrumental sensibility is set by the three components of uncertainty of measurement at the phase detector.

The uncertainty in measuring clean signals, $\Delta \xi_o$, is due either to nonlinearities in the electronics or to the precision in reading the null meter. In the present case, it is the latter and should not vary as long as signal input to the phase detector is maintained. The sensitivity of the meter is $\sim 1.5^{\circ}$/microamp, and since 0.1 microamp may be read easily on the meter scale, $\Delta \xi_o$ is approximately 0.2°.

The second component is that due to noise, which in this case is only the statistical noise-in-signal at the photocathode. This ratio of signal to noise-in-signal is given by

$$S/N = \frac{\bar{i}_s}{\sqrt{2e(\bar{i}_s + \bar{i}_{dc} + \bar{i}_d)\,\Delta f}} \quad , \qquad \text{(C-12)}$$

where e is the electronic charge; the $\bar{i}$'s are average electron currents at the photocathode due to signal (s), dc light (all unmodulated light striking photocathode) (dc), and dark current (d); and Δf is the bandwidth of the particular system used to observe the signal. A number of things should be noted about this equation. First, the noise-in-signal does not depend, except in the way that the dark current varies, upon the current amplification of the tube, but, for a given signal level, does depend on the photocathode quantum efficiency. Second, the noise content of a given bandwidth, Δf in cps, does not vary on heating or translation to a lower frequency. Thus a filter with a 5-cps bandwidth at 1 kc ($Q = 200$) passes the same amount of noise as a 5-cps bandwidth filter at 5 Mc which would have to have a Q of 10^6. Finally, $\bar{i}_{dc}$ and $\bar{i}_d$ should both be made much smaller than $\bar{i}_s$.

For a given noise level, the value of $\Delta \xi_{noise}$ may be reduced in either of two ways. One possibility is to reduce the value of Δf

in Eq. (C-12) by means of narrow band-pass filters. At present, the bandwidth of the electronics up to the phase detector is 125 cps (Q = 8). The implications of narrower bandwidth filters will be discussed under $\Delta \xi_{\text{frequency}}$.

At present, however, the uncertainty due to noise is controlled mainly by using a null meter with a long time constant of 1 sec. Since the noise-in-signal is statistical noise and is random, the long time-constant meter has the effect of taking many instantaneous readings and averaging out the fluctuations due to the noise.

The third component of uncertainty in phase measure at the phase detector, $\Delta \xi_{\text{frequency}}$, is caused by the effects of frequency fluctuations on the impedance of tuned circuits and is the price of reducing noise with narrow band-pass filters. The relation between phase and frequency uncertainties is given by

$$\Delta \xi_{\text{frequency}} \cong K\, 90 \quad \frac{\Delta f}{BW} \qquad \text{(C-13)}$$

where ξ is in degrees, Δf, the uncertainty in frequency, is less than BW/2, BW is the bandwidth, and K is a constant characteristic of the instrument.

The constant, K, in Eq. (C-13) should be much less than unity. The expression with K equal to unity is the shift in phase caused by the change in the impedance of a single tuned circuit due to a change of frequency. Thus, a change in frequency of 0.1 cps, the uncertainty of the frequency standard, produces a 2° phase shift across a tuned circuit with a bandwidth of 4 cps. However, if filters in both the "reference" and "sample" channels were identical within 10%, then the change in phase across each filter would be within 10% of each other

and the change in phase observed by the detector would be reduced by a factor of 10. Furthermore, if the time constant of the phase detector is sufficiently long that the effect of fluctuations of frequency is averaged out, then the effective value of Δf becomes smaller than 0.1 cps.

If necessary, the uncertainty of frequency itself could be reduced by the use of an improved standard. The signal from a crystal-controlled 100-kc oscillator when frequency-divided to 1 kc can be constant to 0.001 cps, an improvement of 10^2.

This assessment of the phase shifts caused by frequency uncertainty shows that narrow band-pass filters are quite feasible. Should the instrumental bandwidth of 125 cps be reduced to 4 cps by Q-multiplier filters, Eq. (C-12) indicates that the signal-to-noise ratio is improved fivefold.

Bonch-Bruevich and Molchano[36] give a useful discussion of noise in similar apparatus.

Possible Systematic Errors

It is useful to list some of the opportunities for malperformance of the apparatus. The nonhomogeneity in phase of the modulated light beam already has been discussed in Section B under "Modulator." Variation in transit time of electrons from the photocathode to the first dynode can be quite serious. This depends on the point of origin on the photocathode, on the accelerating potential, and on the space charge built up by the beam of electrons (signal level). Nonlinearities of the electronics can be serious if any of the circuits are overloaded. Electrical alignment and inter-channel coupling must be checked constantly.

These effects are overcome partially by maintaining exactly the same conditions for measurements on the reference sol and the fluorescer. The

geometry and the size, shape, and orientation of the cell must be the same. The part of the light beam sampled by the reference photomultiplier must be the same as that of the sample. The amount of light striking the sample photomultiplier should be constant during the entire run, and by no means should the photomultiplier potential be changed. Only if necessary to avoid nonlinearities in the electronics should the compensated gain control in the sample channel be used. Phase splitter balance, interchannel coupling, and the ability to measure time of flight of light should be checked before and after each run.

Because of the necessity of reproducing experimental geometry, scattered exciting light is particularly noisome and tends to make the observed phase shift systematically too small. However, the effect may be measured by using a blank cell, and if not too large, a correction can be added to the observed phase shift by means of vector addition.

Apparently various disagreements in the literature are caused also by impure or unknown samples, by too great an actual absorption at the peak (entrapment of radiation), and by depopulation by unknown non-radiative paths.

Experimental Tests of Sensibility and Accuracy

In this section are described tests of the sensibility and accuracy of the apparatus made by measuring the time of flight of light with low-level signals, and the time of flight of electronic signals in cable.

Experimental

Light from an A100-H4 mercury-vapor lamp operated at ~ 1.2 amps dc passed through the optical system shown in Fig. 2 with Lens 2 masked to give a system aperture of f 12. Slit 2 was 1.5-mm wide and 2-mm high.

Sixty-four percent of the green light passing through Slit 2 was modulated.* After Slit 2, a Wratten 77 filter passed only the λ 5461 A line to a fourth lens which produced a parallel beam. This entire light beam passed first through the "reference" scatterer, which attenuated the light by a factor of 2, then through neutral filters with additional variable attenuation up to 10^4 (measured with a Cary Model-11 spectrophotometer). It was then reflected through a U turn by two front-surface, movable mirrors each set at 45° to the direction of propagation of the light beam and finally entered a completely diffuse scatterer directly in front of the "sample" photomultiplier.

The front-surface mirrors were mounted on a 125-cm optical bench parallel to the beam which allowed the path length of the light to be varied 250 cm measurable to $\pm$ 0.04 cm.

RCA-6655 photoelectron multiplier tubes run at 1000-v detected the light. The electronic system had a bandwidth of 125 cps, and the phase detector a time constant of $\sim$ 1 sec.

The test oscillator was controlled by the same crystal used to control the modulator, and the 5.2-Mc harmonic was selected by tuned circuits. The fixed phase shifts of $\sim 3^\circ$, 20°, and 80° associated with the oscillator were calibrated either by measuring a Lissajous pattern on the oscilloscope with identical amplifiers for horizontal and vertical signals (X-Y oscilloscope), or by measuring the cable length necessary to produce an equivalent delay and using the propagation

---

*Cf. Section B, Modulator.

constant given by the manufacturer. The absolute accuracy at best is 5%, but since the cable characteristic does not change with time, non-linearities in the electronics and changes that may occur from run to run may be checked to the maximum sensibility of the apparatus.

Results. The sensibility, which as the preceding discussion has indicated is related to the sensibility, $\Delta \xi$, of the phase detector, was measured with no neutral filters attenuating the light passing through Slit 2, and with attenuation of 10^4 of the light reaching the "sample" photomultiplier. In the first case, the sensibility was ascertained to be 0.2° and is called $\Delta \xi$. With the 10^4 attenuation of the light, the signal-to-noise ratio at the phase detector as observed on an oscilloscope was between 1/2 and 1/5, but the null could be estimated within 0.5° on a single-reading basis. This is then a value of $\Delta \xi_o + \Delta \xi_{noise}$. Most of the noise observed was due to stray, unmodulated light in the room and to photomultiplier dark current.

With the unattenuated green line reaching the "sample" photomultiplier, phase delay caused by changing the light pathlength 200 cm (equivalent to 0.67×10^{-8} sec or 12.6°) was measured to 0.2°. This result is interpreted as a check of the calibration of the phase-shift network in the apparatus and was reproduced at a number of settings of the "reference" and "sample"-channel phase shifters.

When the light level reaching the "sample" photomultiplier is attenuated by 10^4, it approximates the signal level from a fluorescing molecule, such as iodine. This attenuation when the molecule is used is analyzed as follows: Of all the energy in the 5461 A line that strikes the diffuse scatterer in front of the photomultiplier, only 1% would be absorbed by the gas sample if the spacing between lines were

five times the Doppler width. Of this energy, only 1/10 to 1/100 might appear in fluorescence wavelengths to which the photomultiplier is sensitive, hence a total attenuation of 10^4. With this signal level, delays introduced by changing the light pathlength could be measured within the sensibility of the phase detector of 0.5°. This is interpreted as evidence for no interchannel coupling or extraneous signal.

A Phazor 200A phase meter was used for some measurements.* Its accuracy and sensibility were useful for clean signals. However its amplifiers were saturated by the noise components of the noisiest signals measurable by the phase detector in the apparatus.

Tests with the test oscillator and cable delay lines support the results of measurement of time of flight of light. In addition they indicate that the electronic system alone is not sensitive, within its linear range, to changes in signal amplitude. This was most useful in isolating the cause of the large phase shifts described in Section B under "Modulator", and phase shifts due to changing the potential of the photomultiplier supply.

Summary and Conclusions

The uncertainty in measurement of lifetime has been related to uncertainty in phase angle by Eqs. (C-5) and (C-6) and is shown to be limited by the sensibility of the phase detector. Making the phase detector more sensible by narrowing the bandwidth of the electronics is evaluated. Causes of systematic errors have been listed.

Experiments show that the accuracy with signal level comparable to the fluorescence from a gas-phase molecule, or 10^4 smaller than that

*Industrial Test Equipment Co., 55 E. 11 Street, New York 3, N. Y.

from a diffuse scatterer, is within the sensibility of 0.5^{o}. Equation (C-6) indicates that lifetimes from 6×10^{-9} sec to 10^{-7} sec could be measured within 20%. However, the limit at long lifetimes probably is shorter because the signal level decreases according to Eq. (C-4) as lifetime increases.

Part I

D. ACKNOWLEDGMENTS

I am grateful to Professor Leo Brewer for directing my graduate training and for suggesting this problem. His continued interest and many suggestions have greatly added to this work and enriched my experience.

I have had many valuable discussions with Professors W. D. Gwinn and R. J. Myers on the electronics and on the lifetime measurements.

Mr. Jerry M. Sakai of the Lawrence Radiation Laboratory Electronic Engineering group has redesigned and rebuilt the electronic part of the apparatus built originally by C. Geoffrey James, Kenneth Lamers and Richard G. Brewer. Discussions with him and his innovations have been very valuable.

The craftsmen and technical people of the Chemistry Department and of the Lawrence Radiation Laboratory have contributed greatly of their skill and patience toward the culmination of this work. In particular I would like to thank Mssrs. Edward Fleischer, David Millburn, Daniel O'Connell, Harry Robinson, and Robert Waite. Mrs. Jane Waite has provided outstanding secretarial service.

The author is indebted to the National Science Foundation for predoctoral fellowships during 1956-59, and to the United States Atomic Energy Commission for other support of this project.

REFERENCES

1. G. N. Lewis, M. Randall, K. S. Pitzer, and Leo Brewer, Thermodynamics, (McGraw-Hill, New York, N. Y., To be published).

2. E. F. Worden, High-Intensity Light Sources (Part II of thesis), UCRL-8509, October 9, 1958.

3. T. Förster, Fluoreszene Organishe Verbindungen, (Vanden hoeck and Ruprecht, Göttingen, 1951).

4. A. C. G. Mitchell and M. W. Zemansky, Resonance Radiation, (Cambridge University Press, Cambridge, 1934).

5. P. Pringsheim, Fluorescence and Phosphorescence, (Interscience, New York, 1949).

6. See Mitchell and Zemansky[4] or, for example, Ostrovskii, Penkin, and Shabanora, Izvest. Akad. Nauk, S.S.S.R. Ser. Fiz. 22, 729 (1958).

7. H. Kopferman and G. Wessel, Z. Physik 130, 100 (1951).

8. Bell, Davis, King, and Routly, Astrophys. J. 127, 775 (1958); ibid 129, 437 (1959); theses by G. D. Bell (1957) and M. H. Davis (1955), Department of Physics, California Institute of Technology, Pasadena.

9. C. W. Allen and A. S. Asaad, Chem. Abstr. 50, 16396f (1956); ibid 51, 15262d (1957).

10. E. Becquerel, La lumière, ses causes et ses effets (Gautier-Villars, Paris, 1867).

11. For a review of the use of Kerr cells as shutters, see J. W. Beams, Rev. Sci. Instr. 1, 78 (1930); Zarem, Marshall, and Poole, Trans. Am. Inst. Elec. Engrs. 68, 1 (1949); Rev. Sci. Instr. 21, 514 (1950); Baird Atomic Technical Data, R-D 501-1 (1955), B. H. Billings, J. Opt. Soc. Am. 39, 797 (1949), ibid 39, 802 (1949), ibid 42, 12 (1952); R. O'B. Carpenter, J. Opt. Soc. Am. 40, 225 (1950); J. Acoust. Soc. Am. 26, 1145 (1953).

12. E. Gaviola, Z. Physik 42, 853 (1927).

13. W. Szymanowski, Z. Physik 95, 45 (1935).

14. O. Maercks, Z. Physik 109, 685, 589 (1938).

15. K. Ziock, Z. Physik 147, 99 (1957).

16. N. A. Tolstoi et al., Uspekhi Fiz. Nauk 41, 44 (1950); Doklady Akad. Nauk S.S.S.R. 102, 935 (1955); Izvestia Akad. Nauk S.S.S.R. 20, 584 (1956); ibid. 21, 595 (1957).

17. G. Tollin and M. Calvin. Proc. Nat. Acad. Sci. U. S. 43, 895 (1957).

18. Tollin, Fujimori, and Calvin, ibid 44, 1035 (1958).

19. S. S. Brody, Rev. Sci. Instr. 28, 1021 (1957).

20. A. Whetstone, Rev. Sci. Instr. 30, 447 (1959).

21. Heron, McWhirter, and Rhoderick, Proc. Roy. Soc. (London) 234A, 565 (1956).

22. R. B. Bennett and F. W. Dalby, Engineering Department, Radiation Physics Laboratory. E. I. DuPont de Nemours and Co. Inc., Wilmington, Delaware, private communication.

23. G. K. Wertheim and W. M. Augustyniak, Rev. Sci. Instr. 27, 1062 (1956).

24. Clades, Jones, and Wickersheim, Rev. Sci. Instr. 27, 83 (1956).

25. J. W. Beams et al., Science 120, 619 (1954).

26. F. Tsui, Br. J. Appl. Phys. 3, 139 (1952).

27. J. G. Phillips, Department of Astronomy, University of California, Berkeley, private communication.

28. Richard G. Brewer, I. A Method for Determining Radiative Lifetimes of High-Temperature Molecules. II. The Probability of Spontaneous Nuclear Reaction in Molecular Hydrogen (thesis), UCRL-8387, July 21, 1958.

29. Harnik, Many, and Grover, Rev. Sci. Instr. 29, 889 (1958).

30. A. Schmillen, Z. Physik 135, 294 (1953).

31. (a) E. A. Bailey and G. K. Rollefson, J. Chem. Phys. 21, 1315 (1953); (b) E. A. Bailey, Thesis, University of California, 1952.

32. P. Kroman, Thesis, University of California, 1957.

33. L. A. Tumerman, J. Phys. U.S.S.R. 4, 151 (1951); Uspekhi fiz. Nauk 23, 218 (1947) contains a review.

34. A. M. Bonch-Bruevich, Izvest, Akad. Nauk S.S.S.R., Ser Fiz 20, 591, 596 (1956) and

35. A. M. Bonch-Bruevich and V. A. Molchanov, Zhur. Tekh. Fiz. 25, 1653 (1955) (on supersonic grating).

36. A. M. Bonch-Bruevich and V. A. Molchanov, Zhur. Tekh. Fiz. 25, 1825 (1955) (on electronic problems).

37. B. Venetta, Rev. Sci. Instr. 30, 450 (1959).

38. M. L. Nichols and O. J. Thies Jr., J. Am. Chem. Soc. 48, 303 (1926).

39. P. Debye and F. W. Sears, Proc. Nat. Acad. Sci. U. S. 18, 409 (1932).

40. R. Lucas and P. Biquard, J. Phys. Radium 3, 464 (1932).

41. P. Debye, Physik Z. 33, 849 (1932).

42. L. Bergmann, Physik Z. 34, 761 (1933).

43. A. Szalay, Physik Z. 35, 39 (1934).

44. R. Wyss, Helv. Phys. Acta 7, 406 (1934).

45. C. Bochem and E. Hiedemann, Z. Physik 89, 502 (1934); ibid. 91, 418 (1934), and ibid. 94, 68 (1935).

46. H. Falkenhagen and C. Bochem, Z. Elektrochem 41, 570 (1935).

47. C. Bochem, Z. Physik 101, 541 (1936).

48. F. T. Gucher, J. Am. Chem. Soc. 55, 2709 (1933).

49. F. T. Gucher and T. R. Rubin, J. Am. Chem. Soc. 57, 78 (1935).

50. P. Debye, J. Chem. Phys. 1, 13 (1933).

51. Yeager, Bugosh, Hovorka, and McCarthy, J. Chem. Phys. 17, 411 (1949).

52. R. Bär, Helv. Phys. Acta. 8, 591 (1935).

53. C. V. Raman and W. S. Nagendra Nath, Proc. Indian Acad. Sci. 3, 119 (1936).

54. W. G. Cady, Piezoelectricity (McGraw-Hill, New York, 1946).

55. P. Brown and S. Frankel, Components Handbook, Radiation Laboratory Series, J. F. Blackburn, ed. (McGraw-Hill, New York 1949), Vol. 17.

List of Symbols Used

Part II

A	Einstein absorption coefficient
B	Einstein coefficient of spontaneous emission
c	Speed of light
C	Number of collisions
E	Energy
EW	Equivalent width
f	Oscillator strength
g	Statistical weight
h	Planck's constant
I	Light intensity
J	Rotational quantum number
k	Transfer rate (with subscript)
k	Boltzmann constant
k_ν	Absorption coefficient
M	Electric dipole moment
N	Concentration
P	Pressure
P	Transfer probability (with subscript)
R	Transition moment
T	Absolute Temperature
v	(also, ν) Vibrational quantum number

List of Symbols Used

Part II

λ	Wavelength
ν	cm^{-1} (wave number), or frequency
ν	(or v) Vibrational quantum number
τ	Lifetime
Ψ	State Wave function

Common Subscripts

e	Electronic
q	Quenching
rot	Rotational
v,ν	Vibrational
T	Energy transfer

II. THE RADIATIVE LIFETIME OF THE B 0_u^+ STATE OF I_2 BY TWO ABSOLUTE ABSORPTION METHODS

INTRODUCTION

The iodine molecule and problems related to its visible absorption system (B 0_u^+ <—— X 0_g^+)[1,2] have been studied so long and extensively, and the system is so accessible experimentally that its radiative lifetime is particularly interesting. However, there seem to have been no conclusive lifetime measurements made on the iodine molecule. The present work yields a lifetime of 5×10^{-7} sec from data for the absorption of the total band system and of a single rotational line. Evaluation of the theory relating absorption to emission leads one to expect that certain possible theoretical errors average out for the level[3] $v' = 26$, $J' = 34$ which alone[4] may be excited by a narrow mercury 5461 A line. By the use of this lifetime, absolute rate constants for quenching and for vibrational energy transfer by collision are obtained.

Nature of the Problem

Because it is so easily produced, iodine vapor has been extensively studied. It is readily contained and is fairly inert. The absorption-band system lies between 4500 and 6500 A, and the readily observed fluorescence is excited by sunlight or by a large number of easily produced atomic lines. Extensive observation of the fluorescence dates back at least to the turn of the century, and determinations of lifetime almost that long. In addition, many rate studies have been carried out using iodine as the subject.

This gives rise to an interesting situation. Because there is so much known about it, iodine is a good molecule for testing a method of

determining absorption coefficients from radiative lifetimes, and what is unknown becomes so much more important. The value of the radiative lifetime is unknown, but is needed to complete knowledge of vibrational-energy transfer and quenching rates. These being known, theories about other processes are tested, and new problems arise.

Section I describes an apparatus for direct measurement of radiative lifetimes. Its primary purpose is determination of absorption coefficients. These will be used for determination of equilibrium constants and of heats of reaction with the aid of the third law of thermodynamics and of accurate knowledge of energy levels.[5] It is therefore quite important that the process of determining absorption coefficients from radiative lifetimes be checked by the complementary determination of a lifetime from an absorption coefficient, hence part of the motivation for this work on iodine. Once one is determining lifetimes, there are many important applications. In particular, there are many measurements on the efficiency of collisions in quenching and in transferring vibrational energy in upper electronic levels. Because the time the molecules spend in this upper state has been unknown, only the relative rates of quenching and transfer could be known. Estimates of the lifetime of the upper level of iodine range from 10^{-6} to 10^{-8} sec. Depending on which extreme one is inclined to favor, either rates of maintenance of unimolecular reaction and dissociation by energy transfer from an energy bath, or third-body recombination and dispersion of sound were made to seem anomalous.

Although iodine is well known, it is not well understood. The hybridization of the energy levels is not known thoroughly because of the (j,j) coupling and is believed to vary rapidly with changing internuclear distance. Calculation of a transition probability, hence of

a lifetime, by the use of a given wave function and comparison with experiment would be a good test of the wave function. Furthermore, comparison of the lifetime from the absorption with directly measured values for several bands constitutes a check of the variation of wave function with internuclear distance, and hence of the sum rules for transition probability.

Review of Measurements of Iodine Lifetime

Determinations of the iodine lifetime have at least a 40-yr history. Stern and Volmer used self-quenching data and assumed that the quenching cross section equaled the gas kinetic cross section to obtain a lifetime of about 10^{-6} seconds.[6] Stevens[7] used Stern and Volmer's equation and the self-quenching coefficient of Arnot and McDowell[8] to obtain a value of 1.6×10^{-6} sec. Rice used iodine-atom three-body recombination rates to calculate a vibrational energy transfer cross section equal to the ordinary "gas kinetics" value.[9]

Tolman[10] used the data of Fuchtbauer[11] for the absorption of iodine vapor at 5461 A to calculate a lifetime of 3×10^{-3} sec. Apparently, Tolman did not take into account the partition function in calculating the population of the absorbing level. In addition, the measurements were made at 1 mm I_2 pressure and the measuring technique is not clearly stated. Also, the given halfwidth would indicate a large number (10^1 to 10^2) of I_2 lines. Luck estimated an f value of 7.45×10^{-7} ($t = 6 \times 10^{-3}$ sec) for an individual rotational line from his absorption data, but he also apparently did not correct for the distribution of molecules between states.[12] Malamond and Boiteux have studied the reversal of a single rotational line to get an A

value of 2×10^5 sec^{-1} for the $v' = 26 \longrightarrow v'' = 3$ transition.[13] However, they specify neither their values for vapor pressure, partition function, nor broadening by self-quenching, hence this value must be treated as suspect.

Hupfeld obtained directly a value of 1×10^{-8} sec by means of a fluorometer phosphoroscope using Kerr-cell shutters.[14] However, Pringsheim (Page 212, Sec. 71) comments that Hupfeld's measurements of 10^{-8} sec for Na_2 do "not seem to be quite reliable" and does not make reference to them at all in his discussion of the iodine lifetime.[15] Pringsheim does not explain his comment.

Pringsheim (Page 212) mentions also, that the displacement of fluorescence in a molecular beam and broadening of a sharply defined fluorescent beam by Brownian motion sets a limit on lifetime of no longer than 1 μsec.[15]

Rabinowitch and Wood[16] (Footnote 9, Page 362) and Polanyi[17] point out that theoretically the $^3\Pi - {}^1\Sigma$ transition of iodine is analogous to the $^3P - {}^1S$ transition in the Hg, Cd, Zn series and thus argue for an analogous lifetime of 10^{-7} sec. Heil,[18] quoted by Pringsheim (Page 213), explains the high self-quenching efficiency of iodine by a lifetime much longer than the commonly assumed 10^{-8} sec due to the triplet-singlet nature of the transition.

Mulliken has calculated a B value for the entire $^{1,3}\Pi - {}^1\Sigma$ transition[19] and compares it with one obtained from integrated absorption coefficient data by Rabinowitch and Wood[21] over the entire band system between 4500 and 6500 A. These measurements would have been far off of the linear curve of growth of the integrated absorption, as undoubtedly were the values of earlier workers cited by them,[21] had the lines not

been broadened with argon, helium, or air. This raises some question about the validity of their measurements for the unperturbed molecule (see Sec. C, Theory and Discussion). The B value calculated from these data by Mulliken is larger than his theoretical value, and the discrepancy is ascribed to Case-c coupling effects. Neither Mulliken nor Rabinowitch and Wood had calculated a lifetime from these data. Similarly, Sulzer and Wieland observe between 423 and 1423° K the absorption coefficients for the visible and red systems, but give neither f values nor lifetimes.[22]

B. MEASUREMENT OF THE I_2 VISIBLE ABSORPTION

Introduction and Review

Although there are a number of determinations of the visible absorption of iodine already reported in the literature, both external and internal disagreements among the papers indicate the necessity of the present work. It agrees with the previous determinations of the total band absorption but disagrees with Luck's measurement of attenuation of the 5461 A line.[12]

The total band absorption was measured by Rabinowitch and Wood at room temperature with and without foreign gas present,[21] and at higher temperatures without foreign gas by Sulzer and Wieland.[22] While the Rabinowitch and Wood data show no enhancement by foreign gas on the red slopes of their absorption peak, where it would be expected because of the discrete nature of the spectrum, they agree with the theoretical equation of Sulzer and Wieland and with the present measurements. On the other hand, while showing enhancement of absorption all along the red slopes of the absorption, the present measurement does not corroborate the work of Kondratjew and Polak,[23] and of Loomis and Fuller[24] who observed selective enhancement by foreign gas at various points on the red side. The more sensitive test for the selective enhancement of absorption -- placing iodine in vacuum in one beam of a double-beam spectrophotometer and iodine with a foreign gas in the other -- is yet to be performed.

Measurement by Luck[12] of the attenuation of the mercury green line by iodine in the presence of various pressures of nitrogen at 483° K give a result that is higher than that predicted by Sulzer and Wieland's formula.

Dlugosch,[25] Kohler[26] and Harding[27] also have measured iodine absorption. Kohler measured the attenuation of the green line from what seems to have been a hot mercury arc. He finds no enhancement of absorption by argon at 82 mm Hg, although his conditions were such that he was off of the linear curve of growth.* He reports also that fluorescence excited by the yellow mercury lines is quenched more efficiently than that excited by the green line (cf. Alentsev[28]). Dlugosch is quoted in Kohler's paper as having observed that a small part of the iodine absorption is continuous. If this were from another level, it would make the calculated transition probability for the B level greater than it should be. However, this continuum has not been seen in the present measurements, making it less than 20% of the line absorption. Harding measured attenuation of a hot mercury green line by iodine in a cell at 115°C with the iodine pressure controlled by a cold side arm. He observed that helium at about 2 mm Hg produced little enhancement of absorption.

Experimental Technique

The present band-absorption measurements were made with a Cary Model-14 spectrophotometer with about 20 A instrumental width at a wavelength of 5461 A. Because no change in the features resulted from going from 5 to 2-1/2 A/sec scan speed, the latter was used.

---

*Cf. discussion of "Equivalent Width" in Section C, "Theoretical" and References 31, 37, and 39 to 42.

Single-line absorption was measured with a Fabry-Perot interferometer kindly lent by Professor F. A. Jenkins of the Physics Department. The plates were quartz, with a dielectric coating and a reflectance of about 98%, and were sufficiently flat that, with some masking, the instrumental width was 1/20 of an order. A 2.03-mm spacer gave maximum resolution without excessively overlapping the orders, which were separated by about 2.46 cm^{-1} (= 0.74 A). The arrangement was such that either the interference fringes or a calibrated step-weakener could be focused on the plate by means of a 50-cm-focal-length camera. The step weakener was illuminated by only the green line and was projected into the camera by means of a 45-deg mirror.

Eastman Kodak IVF plates were used; exposure time for the fringes was 20 min when didymium glass and Wratten 77 and 61 filters were in the light train. Neutral filters were used in the light train for the calibration so that exposures for both fringes and step weakener were exactly equal. Development was in D-19 for 1 1/2 min at 23°C, with gentle brushing to avoid Eberhard effect.

A microdensitometer* was used to read the plates, each of which bore its own intensity calibration marks.

---

*Made available by Professors F. A. Jenkins of the Department of Physics and J. G. Phillips of the Department of Astronomy.

Iodine for the vacuum cell, used for both single-line and band measurements, was Baker reagent grade (99.8% pure), triply distilled in vacuum and sealed into a Pyrex cell. The measurements with foreign gas were made on iodine without further purification in the presence of air at 1 atmos. Pressure of iodine was inferred from temperature measurements with a precision thermometer and the thermodynamic data of Stull and Sinke:[29] $\text{Log}_{10}P = -3.325$ at 300° K; $\Delta H_{vap} = 14.872$ kcal; $\Delta C_p = 4.34$ calories/deg at 300°K. When data was available the results of other workers were corrected to these values.

The light source for the interferometric measurements was a General Electric A100-H4 medium-pressure (10 atmos under normal operating conditions) mercury-vapor lamp operated with a 0.6-amp current supplied by a Sorenson line regulator. Six iodine lines were covered by this line, but only two were on parts of the mercury line that were flat enough to be measurable.

Of the previous experimenters, Rabinowitch and Wood used iodine at 19° C (p = 0.18 mm Hg) and a 12-cm quartz cell.[21] Their foreign gas was either He, Ar, or air at 500 mm Hg pressure, all of which gave the same results. They report no further enhancement of absorption by higher pressure. Both Sulzer and Wieland, (SW)[22] and Luck[12] used weighed amounts of iodine in cells of varying path lengths. At the higher temperatures, SW corrected for the dissociation of iodine, which did not prove necessary under Luck's conditions. The results of SW are for a range of temperatures from 423 to 1423°K, while Luck worked at 483°K. SW measured the absorption photographically over the whole band system, while Luck measured photoelectrically the attenuation of a presumably narrow mercury green line. Malamond and

Boiteux[13] used a Fabry-Perot interferometer (90% reflectance coatings, 48 and 96-mm spacers) crossed with a prism spectrograph to measure the line shape of the fluorescent lines. From this line shape, they infer the amount of self-absorption. They specify neither temperature, nor path length, nor source of vapor-pressure data.

Results

The results of the various absorption experiments as well as values of interest that have been calculated from them are presented in Tables I through IV. Table I presents the results of the measurements of the total visible absorption of iodine. Sulzer and Wieland's theoretical equation fits the experimental curves quite well, except that the band heads caused irregularities in the absorption and the theoretical points were slightly high far to the red of the absorption peak. Equation (B-1) plus the experimental-peak height was used in calculating the area under the curve. With foreign gas present, the curve to the violet of the continuum onset corresponded exactly to that with no foreign gas, whereas there was enhancement of absorption in the discrete region of the spectrum extending almost the full length to the red of the absorption. The band-system maximum was enhanced more than the red slope, and individual band heads showed greater enhancement at their maxima than at the minima.

The first column of Table I shows the numerical results of these measurements. Values in the second column are calculated from the data of Rabinowitch and Wood. Rabinowitch and Wood's data show no enhancement in either the continuum or lower red slopes of the absorption upon addition of the foreign gases in excess of 500 mm Hg.

Table I

Integrated absorption of the entire visible band system of I_2

Conditions			I	II	III[a]	V[b]	VI[b]	
Temp. (°K)	I_2 press.	Foreign gases	$(\text{Log } \frac{I_o}{I})_{max}$	$\bar{\xi}_{max}$ x 10^{-2} ($\log_{10}$) $\left(\frac{1}{m - cm}\right)$	$\bar{\xi}^t_{max}$ x 10^{-2} ($\log_{10}$) $\left(\frac{1}{m - cm}\right)$	f x 10^2	τ x 10^7 sec	Ref.
302	satd	air at 1 atmos	0.17	7.3	7.5	1	5.0	
292	satd	He, Ar, Air } 500 mm	0.14	7.1	7.6	0.97	4.6[c] 4.6[c,d]	21
423-1323	varies	none				1.1	4.2	22
483	unsatd	N_2 0-1 atmos		(7.4)[e]	5.7		(3.2)	12

[a] Obtained by using Sulzer and Wieland's[22] formula and constants.

[b] Corrected, when necessary to Stull and Sinke's vapor pressures.[29]

[c] λ = 5461.

[d] Obtained from plot of $\bar{\xi}$ vs log ν.

[e] Calculated from the measurement at λ5461 by using Sulzer and Wieland's formula.

The third column presents results of the very extensive measurements of Sulzer and Wieland.[22] Their theoretical formula is:

$$\xi_T(\nu) = \xi_0^M(\tan \Theta/2T)^{1/2}\exp - (\tan \Theta/2T)\left(\frac{\nu - \nu_o}{\Delta\nu_o^*}\right)^2 \qquad \text{(B-1)}$$

where $\xi_T(\nu)$ is the molar extinction coefficient (logarithm to the base 10) for given temperature T and wave number ν. For iodine, Θ is 1.439 times the ground-state vibration frequency (214.5 cm^{-1}); T is the absolute temperature; $\Delta\nu_o^*$ is 1.42×10^3 cm^{-1}; and ξ_0^M is 995.

Since it fits their data quite well and describes a curve enclosing constant area, Eq. (B-1) was used to obtain a value of the transition moment representative of all of SW's measurements.

The fourth column shows values calculated on the basis of Luck's measurement of the attenuation of the 5461 A line by unsaturated iodine at 483° K. in the presence of nitrogen.[12] The band absorption is calculated using only the shape of Sulzer and Wieland's curve and assuming that the maximum absorption is at 5200 A. It is observed that the absorption is 30% greater than that predicted by Sulzer and Wieland's equation. This discrepancy is not explained by the presence of a band head, since extrapolation of Rosen's[30] Deslandres tables indicate none at λ5461 A. However, since large intensity fluctuations over small wavelength regions can be averaged out by low-resolution instruments, the attenuation of the narrow green line (hyperfine structure resolvable) from a germicidal lamp was measured. In order to make this measurement, the germicidal lamp was substituted for the regular tungsten filament source of a Cary spectrophotometer. The extinction so measured was exactly the same as that measured with the regular continuous source.

The best value for the lifetime from these measurements is 5×10^{-7} sec, with $\lambda = 5461$ A. As the discussion section will indicate, it is believed that the theoretical uncertainties are within the experimental uncertainty of $\pm$ 20%. The best value of B, the Einstein transition coefficient, is 1.6×10^{13} cm^2 erg^{-1} sec^{-1} (units of isotropic energy intensity).

Table II shows results for the measurements of the single rotational line. As can be seen from the estimated values of the absorption at the line center, the results are far from the linear curve of growth (see Section C) and set only a lower limit for the absorption coefficient. The experimental uncertainty for the measurement at ice temperature is quite large because of the uncertainty of superimposing the curve for the mercury line without iodine absorption on that for the line with absorption. Comparison with the theoretical curve of equivalent width given by van der Held[31] indicates that the results at the lower temperature are about one order of magnitude lower than the extension of the straight-line curve of growth.

Table III presents a summary of all of the results available for the measurement of a single iodine line, plus values for the total transition probability based on Table IV. All values should be treated as being quite uncertain. The present measurements are off of the linear curve of growth. Luck's value is based on estimates of the number of lines covered and extrapolation to the true profile of the line of the measurement with high optical density and with foreign gas present. Apparently it does not include a correction for the partitioning of the iodine molecules between the various energy levels. This correction was made in the present work on the basis of a rotational

Table II

Absorption by the I_2 line ($B\ 0_u^+$, $v' = 26$, $J' = 34 \longleftarrow X\ 0_g^+$ $v'' = 0$, $J'' = 33$), using a 4.52-cm cell

Temp., side arm ($^\circ$K)	Temp., ambient ($^\circ$K)	Pressure[29] (mm Hg)	EW x 10^{-2} (cm^{-1})	Absorption at center of line[a] observed $\frac{I_o - I}{I_o}$	true	$A_{26\text{-}0}$[b] x 10^{-4} (sec^{-1})
288	300	0.12	1.1	0.19	~ 1	1.3 ± .5
273	300	0.03	0.33 ± .2	~ 0.06	~ 0.3	1.4 ± 1

[a] Using $\text{Absorption}_{\text{true}} = \frac{\text{Inst Width}}{\text{Doppler Width}} \times \text{Absorption}_{\text{observed}}$.

[b] Using partition function = $Q = 4.3 \times 10^3$.

quantum number of 50, and the corrected value is presented. The Malamond and Boiteux data may be quite reliable, but they do not give the various quantities used in their calculations -- such as vapor-pressure data, partition function, iodine pressure, and self-collision broadening.

In Table IV the first column gives the vibrational quantum number of the lower state of the transition from $v' = 26$. The second column gives population in the lower state relative to $v'' = 0$. The temperature was 273° K and the vibrational quantum was taken to be 215 cm^{-1}. The third column contains the height of the fluorescence peak. Iodine pressure is 3.0×10^{-2} mm Hg. The data is from work of C. Arnot and C. A. McDowell (cf. Reference 8). The author is greatly indebted to them for supplying some unpublished information. The fourth column contains values of the fluorescent intensity corrected for self-absorption. The value for $26' \longrightarrow 0''$ is obtained from the value for $26' \longrightarrow 1''$ and the ratios $25' \longrightarrow 0''/25' \longrightarrow 1'' = 0.11/0.09$ and $27' \longrightarrow 0''/27' \longrightarrow 1'' = 0.08/0.08$. For convenience, the ratio $26' \longrightarrow 0''/26' \longrightarrow 0'$ is assumed to be unity. The fifth column gives values of the fluorescent intensity normalized to $26' \longrightarrow 0'' = 1$. Absolute values of the fluorescent rate constant using Malamond and Boiteux[13] value for $k_{26' \longrightarrow 3''} = 2.0 \times 10^{5}$ sec $\pm$ 80% are given in the last column. Only the value for $26' \longrightarrow 0''$ is shown as the total rate constant is determined directly from the sum of the fifth column. Actually, the relative energies shown in columns III to V have not been converted to quanta. In the case of $v'' = 18$, this amounts to 682/566 (see Pringsheim,[15] Table 23, p. 153 for assignment of wavelengths to the fluorescence lines) or 20% shortening if that line made the major contribution to the rate of depopulation.

Table III

Einstein A coefficients for single rotational lines in the 26' ⟶ 0" band of the iodine visible-band system

Line				A_{line}	A_{total}†	
v'	J'	v''	J"	(sec^{-1})	(sec^{-1})	Reference
26	34	0	33	$> 71.4 \times 10^4$	$\gg 4.5 \times 10^4$	This work
26	34	3	*	$20 \pm 16 \times 10^4$	$200 \pm 160 \times 10^4$	Malamond and Boiteux[13]
*	*	*	*	1.7×10^4	5.5×10^4	Luck[12]

*Not known

†Estimated

Table IV*

Relative fluorescent intensities for 26' ⟶ n" transitions in I_2 visible system

ν	$\frac{N_{\nu''}}{N_{\nu''}}$	I (arbitrary units) peak height	cor-rected	nor-malized	Rate Constant (sec^{-1})
0	1	-	5.13	1.000	(6.29)
1	0.320	1.66	1.90	0.370	
2	0.104	0.00	0	0	
3	0.033	1.63	1.63	0.318	$2 \times 10^5 \pm 80\%$
4	0.011	0.48	0.48	0.094	
5		?	?	?	
6		1.14	1.14	0.222	
7		0.10	0.10	0.019	
8		1.29	1.29	0.251	
9		0.06	0.06	0.012	
10		0.97	0.97	0.189	
11		0.51	0.51	0.099	
12		0.33	0.33	0.064	
13		0.87	0.87	0.170	
14		0.00	0.00	0.00	
15		0.87	0.87	0.170	
16		0.13	0.13	0.025	
17		0.60	0.60	0.117	
18		0.54	0.54	0.105	
		Σ = 11.18	16.55	3.225	$2 \times 10^6 \pm 80\%$

Conversion of single-line absorption data to lifetime requires knowledge of the relative intensities of the fluorescence from $v' = 26$ to the various vibrational levels of the ground state. Table IV presents values for these intensities based on unpublished work of Arnot and McDowell (See Reference 8, however, for experimental details).

The values actually observed by Arnot and McDowell are heights of the fluorescence peaks and are shown in Column III. These were corrected for self-absorption by the use of the relative populations shown in Column II and the results shown in Columns IV and V. The first step in treatment of the data was to obtain a value for the $26' \longrightarrow 0''$ fluorescence intensity. This cannot be determined directly, because the $26' \longrightarrow 0''$ line is masked by scattered light from the exciting source. To obtain this information we have assumed that the transition probability is determined only by the lower vibrational wave function and is independent of whether the upper corresponds to $v' = 25$, 26, or 27. In doing this, we assume that the wave functions of the upper level do not change much with v' for internuclear distances corresponding to good overlap with the lower level. We assume also that they are not displaced from one another (cf. Pringsheim,[15] p. 156). On the basis of this assumption, the intensities of fluorescence depend only on the lower quantum numbers. Data for the transfer bands originating from levels 25 and 27 observed by Arnot and McDowell indicate that the apparent ratio of intensities (26-0) : (26-1) is 1:1.

The data from the Fabry-Perot measurements, Table II, indicate that self-absorption in the fluorescence tube is important. Correction for this is made by assuming that the lines are triangular, and the absorption at the peak (from Table II) is 30% for an $\sim$ 5-cm path length, hence the

energy attenuation over the entire line is 15%, or log $(E_o/E) = 0.07$. For the 70-cm cell used in the fluorescence work, log (E_o/E) is $(14/2)(0.07) = 0.49$, and the intensity without self-absorption is 3.1 times greater than that observed. The remaining lines may be corrected by using knowledge of relative populations (Column II, Table IV) and the method of successive approximations. For the zero-order approximation, the ratio of absorption coefficients is assumed to be unity, and the ratio of logarithms of self-attenuation is equal to the ratio of populations. This gives zero-order corrected intensities which are used as the ratio of absorption coefficients in a first-order approximation, etc. The approximations converge very rapidly.

Lifetimes may be obtained from these relative intensities by combining them with the available absolute-absorption measurements. From the rate constant of Malamond and Boiteux for the 26 $\longrightarrow$ 3 transition indicated in Column VI, a lifetime not including depopulation to $v'' > 18$, of 5×10^{-7} sec is obtained. Depopulation to higher levels probably does not shorten this by more than a factor of two.

The large number of members in the 26' $\longrightarrow$ n" progression seems to constitute a violation of the Franck-Condon principle. Actually, a similar set of maxima in the v'' progression has been observed and explained theoretically in the case of RbH by Gaydon and Pearse.[32] The phenomenon seems to occur when there is a large change in the equilibrium value of the internuclear distance.

Intensity data for the progression beyond the eighteenth member are uncertain. Pringsheim does indicate (Table 26, p. 160) that no fluorescence is observed beyond 6000 A upon excitation with a broad mercury 5461 A line.[15]

Extrapolation of Alentsev's curve,[28] again for broad-band excitation, indicates that intensity beyond 6500 A is small, although he presents no actual data for fluorescence to the red of 6500 A. Oldenberg has examined the progression and gives relative blackening for the members $v'' = 22$ through 37, but he does not relate these to the intensities of the first members of the progression.[33] His measurements show no trend towards decrease of fluorescence intensity with increasing v''. Rank has measured the positions but not the intensities of this fluorescence series.[34]

On the basis of these data we assume that there are no large secondary maxima in the fluorescence intensities and that the accumulated transition probability for the members of the series with $v'' > 18$ is not more than that for the first 19 members. The sum of transition probabilities in Table IV, Column VI, compensated for transitions in the remainder of the series gives a lifetime of 3×10^{-7} sec. This value bears $\pm$ 80% uncertainty from the absorption coefficient, plus the uncertainty in the relative fluorescences.

Summary

A value of 5×10^{-7} sec $\pm$ 20% for the lifetime of the B 0_u^+ level is obtained from integrated band-absorption measurements (Table I). Results from single-line absorption plus relative fluorescence intensities are more uncertain and do not contradict the integrated band absorption results. In view of the large uncertainty in the single-line results, 5×10^{-7} sec $\pm$ 20% is the preferred value.

C. THEORY AND DISCUSSION

Treatment of the Data to Yield Lifetimes

Absorption is related to emission by means of thermodynamic arguments, and to matrix elements of the wave functions by quantum-mechanical arguments. First-order treatment relates the matrix elements to one another and gives rise to the sum rules, which then relate various forms of absorption measurement to the lifetime of the excited levels.

The lifetime obtained is used for several purposes. Comparison is made with a direct determination using the lifetime apparatus. Comparison could be made also with various theoretical predictions. Finally, the lifetime value is used to put measurements of relative energy-transfer cross sections on an absolute scale.

Theoretical

It is possible to relate the various quantities characterizing absorption and emission. The probability of absorption of a photon (Einstein B coefficient) is proportional to the probability of spontaneous emission (Einstein A coefficient). The B coefficient may be related also to matrix elements, to the oscillator strength, f, and to the measured intensity of an absorption. By means of the sum rules, the B value may be related also to the lifetime of a single rotational level or to that of the upper level of a single vibrational band.

Units. Because the experiment involves a flow of energy and since photographic plates are calibrated in terms of energy per unit blackening, we adopt a system using intensity (not density) of radiation in energy units.

Terminology. The probability per unit time that a system will absorb energy and go to a higher state is

$$P = B_{n-m}\, I(\nu_{n-m}) \quad , \tag{C-1}$$

where B_{n-m} is Einstein's coefficient of absorption.

The probability of emission is, per unit time,

$$P\ (\text{emission}) = A_{m->n} + B_{m->n}\, I(\nu_{nm}) \quad , \tag{C-2}$$

where A and B are Einstein's coefficients of spontaneous and induced emission. If there are only radiative transitions, we have

$$\tau = 1/A_{total} \tag{C-3}$$

where A_{total} is the sum of A values for transition to all lower states.

Sometimes it is convenient also to speak of an f value or oscillator strength. This factor, which appeared first in classical theory and relates the intensity of radiation calculated on the basis of an oscillating electron to that actually observed, is

$$f = \frac{\eta}{N} \, , \tag{C-4a}$$

where η is the number of classical oscillators, and N is the actual number of atoms, molecules, etc. The oscillator strength is related to the lifetime by

$$f\,\tau = 1.51\,\lambda^2\ \frac{g'}{g''} \, , \tag{C-4b}$$

where g' and g'' are statistical weights of the upper and lower states, respectively.

The three Einstein coefficients may be interrelated by the use of the theory of microscopic reversibility and Planck's law:

$$I(\nu) = \frac{2h\nu^3}{c^2} \quad \frac{1}{e^{(h\nu/kT)} - 1} \quad \text{(Energy/sec/cm}^2\text{/solid angle/frequency)}$$

Let N_n, N_m be populations of the two states. Then the number going from n to m is $N_n B_{n\rightarrow m} I(\nu_{nm})$, and the number from m to n is $N_m (A_{m\rightarrow n} + B_{m\rightarrow n} I(\nu_{nm})$. At equilibrium we have

$$\frac{dN_n}{dt} = \frac{dN_m}{dt} = 0$$

and

$$\frac{N_m}{N_n} = \frac{I(\nu_{nm})\, B_{n\rightarrow m}}{\left[A_{m\rightarrow n} + B_{m\rightarrow n}\, I(\nu_{nm})\right]} = e^{-h\nu_{nm}/kT} . \qquad \text{(C-6)}$$

We solve for $I(\nu_{nm})$:

$$I(\nu_{nm}) = \frac{A_{mn}}{B_{nm}\, e^{+(h\nu_{nm}/kT)} - B_{mn}} . \qquad \text{(C-7)}$$

By comparison with Planck's equation, we have

$$B_{nm} = B_{mn} \qquad \text{(C-8)}$$

and

$$\frac{A_{mn}}{B_{nm}} = \frac{2h\nu^3}{c^2} \qquad \text{(C-9)}$$

where B is in units of intensity of isotropic radiation. For some purposes it is convenient to have B in energy density units; to convert, we use

$$B(\text{density}) = \frac{c}{4\pi} B\ (\text{intensity}). \qquad \text{(C-10)}$$

The relation between B and the wave functions is given in intensity units by[35]

$$B_{mn} = \frac{32\pi^4}{3h^2c} \left[\int \psi_m^* \; R \; \psi_n \, d\tau \right]^2 \quad . \tag{C-11}$$

where R is the transition moment.

B may be related to the integrated absorption coefficient. Consider a beam of parallel light, $\nu \leq \nu \leq \nu + d\nu$ and $I = I(\nu)$, traveling in the x direction from x to x + dx. There are N molecules or atoms per cm^3 of which δN_ν can absorb I_ν and $\delta N_\nu'$ can emit. Then, by conservation of energy, we have

$$- \delta [I_\nu \, d\nu] = \delta N_\nu \; dx \; h\nu \, B_{nm} \frac{I_\nu}{4\pi} - \delta N_\nu' \, dx \, h\nu \, B_{nm} \frac{I_\nu}{4\pi} \quad . \tag{C-12}$$

When the B's and I_ν's are for isotropic radiation, we have

$$- \frac{1}{I_\nu} \frac{dI_\nu}{dx} \delta\nu = \frac{h\nu}{4\pi} (B_{nm} \; \delta N_\nu - B_{nm} \; \delta N_\nu') \quad . \tag{C-13}$$

Using $d \log I_\nu = - k_\nu \, dx$, we obtain

$$- \frac{1}{I_\nu} \frac{dI_\nu}{dx} \delta\nu = k_\nu \, \delta\nu = \frac{h\nu \, B_{nm}}{4\pi} (\delta N_\nu - \delta N_\nu') \tag{C-14}$$

and

$$\int k_\nu \frac{d\nu}{\nu} = \frac{h}{4\pi} B_{nm} N \left(1 - \frac{g_m}{g_n} \frac{N'}{N} \right) , \tag{C-15}$$

here the g's are statistical weights and are introduced to account for degeneracies. Usually we have $N' \ll N$ and the second term on the right is neglected. Using Eqs. (C-9) and (C-3), we obtain

$$\int k_\nu \frac{d\nu}{\nu} = \frac{Nc^2}{8\pi\nu^3} \frac{g_m}{g_n} \frac{1}{\tau} , \tag{C-16}$$

where ν is in sec^{-1} and N in atoms/cc.

For a number of reasons it is convenient to work with the equivalent width or integrated absorption of the feature,

$$EW = \int \frac{I_o(\nu) - I(\nu)}{I_o(\nu)} \, d\nu \, , \qquad \text{(C-17)}$$

where $I_o(\nu)$ and $I(\nu)$ are the light intensities before and after absorption and may be functions of wavenumber. Equivalent width may have units of wavelength (hence the name), frequency, or wave number. Experimentally, one rarely has sufficient resolving power to measure the integrated absorption coefficient, Eq. (C-16). However, as one would expect from conservation of energy, the equivalent width has been shown experimentally to be independent of the instrumental width of the spectrograph.[36]

Consider the equivalent width of a feature for small absorption. If for simplicity, $I^o(\nu)$ is taken as constant, we obtain

$$EW = \int \frac{I^o(\nu) - I(\nu)}{I_o(\nu)} \, d\nu = \int \frac{I_o}{I_o} (1 - e^{-k_\nu \ell}) \, d\nu \qquad \text{(C-18)}$$

Then for $k_\nu l \ll 1$, e.g. values on the linear curve of growth, we can write

$$EW = 1 - \left[1 - k_\nu \ell \frac{+(k_\nu \ell)^2}{2} \ldots\right] d\nu \cong \int k_\nu d\nu \, . \qquad \text{(C-19)}$$

Thus the equivalent width can be related directly to B or by Eqs. (C-15) and (C-16).

We are interested also in the equivalent width corresponding to larger absorptions when only Doppler and natural broadening are present, the curve of growth starts linearly at the origin with a slope that is directly proportional to the number of absorbers. It then turns over a knee onto a

plateau with very small slope. The length of the plateau depends on the ratio of natural to Doppler widths, increasing in length directly with decreasing ratio. Finally the equivalent width increases proportionally to the square root of absorbers.

A discussion of line shapes and of curve of growth is given by Mitchell and Zemansky.[37] A curve of growth formula ignoring natural width and a nice derivation are given by Davis.[38] More complete formulae and plots are given by Schutz,[39] by van der Held,[31] and by Kavanaugh, Bjornerud, and Penner,[40] and by Elsasser.[31] Penner and Kavanaugh[42] give a curve of growth that takes into account both Doppler and foreign-gas-collision broadening.

One would expect that the iodine lifetime could be obtained from the square-root portion of the curve of growth for extremely high optical density. If the lifetime were 10^{-6} sec, 400 atmos-cm (4 atmospheres pressure of iodine with a 100-cm path length) would be necessary. If the natural lifetime were as short as 10^{-7} sec, only 4 atmos-cm would be needed (the factor of 10^{2} comes from a tenfold increase in absorption per molecule, and from the more rapid onset of the square-root portion of the curve.) Since the collision lifetime is comparable to 10^{-7} sec at 10^{-3} atmos, the low pressures necessary to avoid collision broadening require also prohibitively long path lengths.

On the assumption of separability of electronic, vibrational and rotational energy and of harmonic-oscillator, rigid rotator, sum rules[43] relate absorption of lines and bands to the electronic transition probability.

The B coefficient is related to the transition-moment matrix element by

$$B_{mn} = \frac{32\pi^4}{3h^2c} \left[\int \psi_m^4 \; M \; \psi_n \, d\tau \right]^2, \qquad \text{(C-11)}$$

where m is the electric moment and may be resolved into nuclear and electronic parts M_n and M_e. The integral in Eq. (C-11) is the transition moment, denoted by R^{mn}, and its square is the transition probability.

If we have

$$E = E_e + E_\nu + E_{rot.} \qquad \text{(C-20)}$$

then we can write

$$\psi = \psi_e \, \psi_\nu \, \psi_{rot.} \quad , \qquad \text{(C-21)}$$

and it can be shown that

$$B_{nm,\nu'\nu'',j'J''} = \frac{32\pi^4}{3h^2c} \left[\int \psi_{e'}^n \, M_e \, \psi_{e''}^m \, d\tau_e \int \psi^{\nu'} \, \psi^{\nu''} \, d\tau_{\nu ib.} \right.$$

$$\left. \frac{\sum_{M'M''} \int \psi_r^{J'} \, \psi_r^{J''} \, d\tau_{rot.}}{2J+1} \right]^2 \qquad \text{(C-22)}$$

$$= \frac{32\pi^4}{3h^2c} \; | \, R_e^{nm} \, |^2 \; | \, R_{\nu ib.}^{\nu'\nu''} \, |^2 \; \frac{\sum_{M'M''} | \, R_{rot.}^{J'J} \, |^2}{2J+1} \quad , \qquad \text{(C-22)}$$

Where the choice of J in the denominator depends on whether one is concerned with emission or absorption.

The sum rules state:

$$\sum_{J'M'M''} | \, R_{rot.}^{J'J''} \, |^2 = 2J'' + 1 \qquad \text{(C-23a)}$$

$$\sum_{J''M'M''} | \, R_{rot.}^{J'J''} \, |^2 = 2J' + 1 \qquad \text{(C-23b)}$$

$$\sum_{\nu'} \left| R_{\nu ib.}^{\nu'\nu''} \right| = \sum_{\nu''} \left| R_{\nu ib.}^{\nu'\nu''} \right| = 1. \qquad \text{(C-24)}$$

Using Eqs. (C-13), (C-14), and (C-15), we obtain

$$B_{nm} = \sum_{\nu'J' \text{ or } \nu''J''} B_{nm,\nu'\nu'',J'J''} = \frac{32\pi^4}{3h^2c} \left| R_e^{nm} \right|^2 . \qquad \text{(C-25)}$$

From Eq. (C-9),

$$A = \frac{2h\nu^3}{c^2} B ,$$

we have

$$\frac{1}{\tau} = A \frac{2h}{c^2} \sum \nu^3 B = \frac{64\pi^4}{3hc^3} \sum_{m\nu''J''} \nu^3_{nm,\nu'\nu'',J'J''} \left| R_e^{nm,\nu'\nu'',J'J''} \right|$$

$$= \sum_{m\nu''J''} A_{nm,\nu'\nu'',J'J''} \qquad \text{(C-26)}$$

$$\cong A = \frac{64\pi^4}{3hc^3} \nu^3 \left| \bar{R}_e \right|^2 , \qquad \text{(C-27)}$$

if in Eq. (C-26) ν does not vary considerably and where $\left| \bar{R}_e \right|^2$ is an average value of the electronic transition probability.

Lifetime from Total Band-Absorption Data.

Since the law of microscopic reversibility was invoked in deriving the relation between the Einstein A and B coefficients, a necessary condition on our work is that only mechanisms complementary to the observed adsorption, and all of these, be active in depopulating the excited state. Experiment and selection rules confirm this. However, the numerical value of lifetime still involves the uncertainty of the

sum-rule assumption that the electronic-transition moment is small and that the variation in the ν^3 term of Eq. (C-26) likewise is small. The assumption is examined and predicted to be small and means of correcting for the ν^3 variation are indicated.

Processes involved in the absorption and fluorescence. In order that the measurement of total band absorption yield a true natural lifetime of the B 0_u^+ state of iodine, certain conditions must be met. First, the process responsible for the observed absorption must be only the transition between the X (ground) and B states. Second, the decay may be complementary only to the absorption observed; decay to another electronic level or decay by predissociation would make the true lifetime shorter. Finally, the presence of foreign gas must not enhance the transition moment.

It seems unlikely that more than one electronic transition was observed in the work on the single line. Separation between lines and observed widths were such that each line was resolved from its neighbors. If the continuum reported by Dlugosch[25] were present, an upper limit to its intensity could be set at one-third of the line absorption, this being the estimated limit of observation of the present work. Apparently Dlugosch herself estimates it to be still smaller.

Contributions from the other members of the states Π and $^3\Pi$, of which B, the upper state of the visible-band system is considered to be a member, are negligible according to calculations by Mulliken.[20] Sulzer and Wieland[22] have measured the areas under the absorptions to the B and A levels and report a 20 : 1 ratio.

Other states that might contribute to the integrated-band-system absorption are those arising from the unexcited atoms: 1_u, 0_g^+, and 0_u^-. The first, 1_u, is included in Mulliken's calculations; the second is the

ground state itself; and the third is forbidden to combine by the selection rule that plus shall not combine with minus.

In iodine, fluorescent decay to electronic levels other than the ground state is forbidden. For other molecules to be studied with the lifetime apparatus, energy levels will have to be worked out and transition probabilities ascertained either by use of selection rules or by measuring relative fluorescent intensities. Should this experiment be necessary, it would be also a nice way of discovering and characterizing previously unobserved electronic states.

Spontaneous predissociation of the iodine molecule does not seem likely. Selection rules forbid it, and the relative fluorescent yield does not vary with variations in the wavelength of the exciting light.[28] Apropos other measurements to be done with the lifetime apparatus, predissociation would be energetically impossible since in the case of most high-temperature molecules, the upper level of the transition usually falls below the energy of two unexcited atoms.

Two pieces of experimental evidence indicate that foreign gas does not enhance the iodine transition probability. The first refutes early observations showing enhanced absorption in an analogous absorption in mercury. The second is a direct observation showing no enhancement.

Michels, de Kluiver, and Middelkoop[44] have determined the transition probability for the $^3P_1 - {}^1S_0$, λ 2537, transition in mercury as a function of argon density to 450 Amagat. This transition is in many ways similar to the presently observed transition in iodine, including symmetry of states, case-c coupling and oscillator strength. Their results indicate no change in transition probability up to 100 Amagat. Previous results cited by Michels et al show an apparent substantial increase in the

transition probability which is now ascribed to an increase of mercury-vapor concentration caused by the presence of foreign gas.

Definite evidence that the iodine transition is not enhanced by the presence of one atmosphere of air is the observation that the absorption in the continuous region is not enhanced. Further, the quantitative agreement between Sulzer and Wieland's semi-empirical curve[22] and the room-temperature data indicates that I_2 - I_2 collisions do not enhance the transition probability. On the other hand, Rabinowitch and Wood in their Fig. 1 quote data that the molar extinction coefficient on the blue side actually decreases with increasing iodine pressure and temperature. This is suspect.

Sum-rule assumption. On the basis of the sum rules, Eq(C-23) and (C-24), Eq. (C-25) states that the sum of transition probabilities within a given electronic transition is independent of the original vibration-rotation level. The key assumption here is that the electronic transition probability $| R_e^{mn} |^2$ does not change with internuclear distance. Examination of this assumption shows that the transition probability for the 26' $\longrightarrow$ 0" transition should be equal to the average value calculated from the total band absorption data. However another uncertainty arises from the fact that the transition probability is divided among many fluorescence transitions and that the fluorescence rate has a ν^3 dependence as shown in Eq. (C-26).

The most significant weakness of the sum rules is that the electronic-transition moment varies with vibrational level or with internuclear distance. Since in measuring the absorption of the entire band system of iodine we are integrating over all of the vibrational and rotational levels and the continuum, the variation of internuclear distance and hence

of electronic-transition moment is at an extreme. This variation should be very great, since the transition is forbidden for separated atoms and is enhanced by case-c coupling for the united atom. Sayvetz, working in Mulliken's laboratory, has calculated variation of R_e^2 for the halogens. Mulliken reports that the variation is large but presents numbers for only chlorine and bromine.[45]

However, we are in a position to estimate the size of this effect. The electronic-transition moment may be expanded in a series

$$R_e(r) = R_e(\bar{r}_{\nu',\nu''}) + (r - \bar{r}_{\nu',\nu''})\, R_e'(\bar{r}_{\nu',\nu''}) + \frac{(r - r_{\nu',\nu''})^2}{2} R_e''(\bar{r}_{\nu',\nu''}) + \cdots , \tag{C-28}$$

where $\bar{r}_{\nu',\nu''}$ is an internuclear distance characteristic of a transition between the two vibrational levels specified. It is defined by

$$\bar{r}_{\nu',\nu''} = \frac{\int \psi_{\nu'} r\, \psi_{\nu''}\, d\tau}{\int \psi_{\nu'} \psi_{\nu''}\, d\tau} . \tag{C-29}$$

Ignoring higher terms, we obtain

$$R_e(r) = R_e(\bar{r}_{\nu',\nu''}) . \tag{C-30}$$

Using this, we see that the range of $\bar{r}$ in the room-temperature iodine absorption measurements is given essentially by the amplitude of the vibration in the lowest level of the ground state or about 0.2 A. If we use this change in radius and the values of transition probabilities for F_2 and Cl_2,[45] we estimate a change by a factor of two to four over the extremes of the vibrationless level.

It is interesting to consider what might be the effect on individual vibrational transition probabilities should there actually be a large variation of R_e over the band system. The 26' —> 0" transition is near the center of gravity of the absorption, and it is expected that the variation of transition probability would average out to give a correct value. However, there would be a systematic trend in the lifetimes of fluorescences excited by, for example, the Cd λ 5086, the Hg λ 5461 and the Hg yellow lines (cf. Turner[46] for experimental details).

Even though the sum rules state that there is conservation of transition probability, Eq. (C-26) states that the rate constants for depopulation to various lower levels depends on the cube of the energy of the transition. Since the iodine fluorescence is known to extend far to the red, it is possible that the lifetime is thus lengthened. Relative fluorescent intensities, such as those given in Table IV, could be used to correct for this, however the extent of present knowledge of intensities precludes making a significant correction. Because of the ν^3 dependence, the lifetime is one-third greater when 6000 A is used as the center of gravity of the fluorescence-intensity curves of Alentsev[28] than when 5461 A is used.

Lifetime from the Absorption by a Single Line.

Determination of the radiative lifetime of an individual vibrational-rotational state from single-line absorption data plus relative fluorescence intensities is much simpler theoretically than from band data. Because Eq. (C-9) is based only on a thermodynamic argument, it holds rigorously, and gives the rate constant for decay to the original level. Ostensibly, transition probabilities to all other states are determined directly from the fluorescence intensities, and the lifetime is determined with no

theoretical assumptions. In practice, measurement of all of the quantities required is difficult. Although this is tedious in the case of iodine because of the narrowness and close spacing of the lines and because of the wide wavelength range of the fluorescence, it may be even more difficult in other molecules because of the possibility of low-energy electronic transitions.

While this method can give the lifetime of a particular vibrational-rotational level with no theoretical uncertainty, one must invoke the sum rules to infer the lifetime of other levels. This presents all of the difficulties due to variation of the electronic-transition probability with internuclear distance previously discussed. Similarly, if fluorescence distribution over wavelength changes, the ν^3 dependence shown in Eq. (C-26) may become important.

Applications of the Lifetime Measurements

Direct Measurement of Lifetime

One extremely important application of this result for iodine will be to test the method to determine absorption coefficients from direct measurement of lifetime with the equipment described in Part I of this thesis. Iodine is well suited for this check because its vapor pressure is known and because it is easily produced and contained. If the 5.2-Mc modulator were used, the 5×10^{-7} sec lifetime would produce a phase shift whose tangent is 16. This is not measurable, and the measurement should be carried out with the 60-kc modulator, in which case we have $\tan^{-1} \phi = 0.1800$, a convenient although somewhat small value.

R. G. Brewer[47] used a prototype of the present equipment with the 60-kc modulator to obtain a longer limit of 4×10^{-7} sec. However, using Arnot and McDowell's value of 2×10^5 for the ratio of self-quenching

to fluorescence-rate constant,[8] and the lifetime of 5×10^{-7} sec, one obtains a self-quenching "lifetime" of 2×10^{-7} sec at 21°C. At the same time, the self-absorption at the peak of the line is very large, as shown by Table II, Column 6. Thus Brewer's experimental results were made under unfavorable circumstances and do not necessarily disagree with our measurement.

Theoretical Application

At present, theoretical work for comparison with the measured lifetime is very sparse. Mulliken[19,20] has calculated a B coefficient that is smaller than that observed. The discrepancy is attributed to case-c coupling effects in the molecule. Another comparison is the f value for the λ 2537 transition of mercury, which is expected to be similar to that for iodine. The values are 0.026[37] and .008 for mercury and iodine, respectively.

Highly desirable checks on the theoretical sum rules, are determination of the transition probability from the integrated absorption of a single-band progression, e.g. in the red where band overlap is reduced, and direct measurement of lifetime of different vibrational levels of the upper state.

Energy Transfer by Collision

Although the relative rate of quenching and vibrational-energy transfer has been long studied, it has been impossible to calculate absolute rates because of the ambiguity in the iodine lifetime. Absolute rates for self-quenching, quenching, and vibrational-energy transfer by various gases are presented in Table V. These results are in agreement with some other experiments, but pose problems in interpreting certain data on reaction rates.

Table V

Coefficients for vibrational energy transfer and for quenching of excited iodine in the B 0_u^+, $v' = 26$, $J' = 34$ state

Gas	Kinetic radius, r (A)	k_T/k_F Exp't liters $\times 10^{-4}$	k_T/k_F Theoret. $mole^{-1}$ $\times 10^{-4}$	k_T Exp't $\frac{1}{\text{mole-sec}} \times 10^{-10}$	p_T	C_T collisions per transfer	k_q Exp't $l\text{-}m^{-1}$ $\times 10^{-4}$	k_F Theoret. $l\text{-}m^{-1}$ $\times 10^{-4}$	k_q $\frac{1}{\text{mole-sec}} \times 10^{-10}$	p_q	C_q Collisions per quenching	Ref.
			$\tau = 5 \times 10^{-7}$	$\tau = 5 \times 10^{-7}$								
I_2	2.7	0		0	0		20	6.3	40.	3.2	1/3	8,17
He	0.98	5.31	16.2	10.6	0.33	3	3.12	16.2	6.2	0.19	5	8
Ne	1.18	2.69	8.30	5.4	0.32	3						8
Ar	1.46	1.64	6.95	3.3	0.24	4	10.1	6.95	20.	1.4	2/3	8
O_2	0.47	1.5	6.85	3.0	0.22	5						8
H_2	1.1	1.9	25.	3.8	0.076	13	0.84	25.	1.7	0.034	30	8,17
D_2	1.1	2.7	17.5	5.4	0.15	7	1.46	17.5	3.0	0.083	12	8,17

In Table V, k_T is the rate of transfer from the $v' = 26$ state to all other states ($v' = 24, 25, 27$). The experimental value is from the measured ratio of k_T/k_F and the presently determined value of k_F is 2×10^6. The probability per collision that transfer will occur to some other vibrational level is p_T and C_T is the number of collisions needed, on the average, to cause transfer. The theoretical value of k_T/k_F is obtained from Eq. (C-31) is

$$k_T/k_F = \frac{p\tau N(r_1 + r_2)^2}{1000} \, 8\pi RT \left(\frac{1}{m_1} + \frac{1}{m_2} \right)^{1/2} \qquad \text{(C-31)}$$

where p is taken as unity, N is 6×10^{23} moles/liter; m_i are the molecular weights, and r_i are as shown in the table.

As pointed out by Pringsheim in his review (Section 48), the literature on the subject of fluorescence and energy transfer in iodine is far more extensive than that for any other molecule. The presence of bands caused by transfer of the iodine molecule from $\nu' = 26$, $J' = 34$ (to which level[3] alone[4] it may be excited by a narrow mercury green line) by collision with various gases was first observed by Franck and Wood in 1911.[48] Subsequently there have been a number of experiments[8,17,49,50] and calculations[7] on the absolute cross section for transfer and for quenching. In these experiments, the iodine was excited to the given level by a narrow mercury line, and the intensities of fluorescence were measured quantitatively from each of the given upper levels as a function of foreign gas pressure.

Table V shows the results of experiments by various workers using H_2, D_2, He, Ne, Ar, O_2 and N_2. The quenching and transfer cross sections obtained are approximately the same as the gas kinetic, based on the 5×10^{-7} sec lifetime. There is some, but not much, ambiguity caused by the fact that workers not using water-cooled lamps must have excited the $\nu' = 28$ level directly. Thus, as it turns out, the actual rate of vibrational energy transfer was enhanced by about 30%.

Other experiments are in agreement with these values. Dwyer has shown, in an experiment made ambiguous by the cascade of molecules from higher levels, that iodine itself is not efficient in transferring vibrational energy among the levels of the ground state.[51] Rice has used three-body recombination-rate data to calculate a transfer cross section for high vibrational levels about equal to the gas kinetic.[9] Durand,[52] Pienkowski,[53] and Heil[18] have measured the efficiency of transfer and quenching in S_2, Te_2, and Se_2. Durand finds a transfer cross section about equal to the geometric.

Montroll and Shuler[54] have derived an expression for the frequency factor A for the dissociation of a diatomic molecule placed in a high-temperature bath of gas. Their formula is

$$A = Z^* P_{10} (N + 1) (1 - e^{-\Theta})^2 , \qquad (C\text{-}32)$$

where Z^* is the number of collisions per unit time suffered by the molecule when the gas density is one molecule per unit volume, P_{10} is the probability that a collision will induce a transition from vibrational level 1 to level 0, N is the number of discrete levels (approximated by a dissociation energy of 12,000 cm^{-1} divided by a vibrational quantum of 200 cm^{-1}), and Θ is $h\nu/kT$. These authors have calculated A, assuming P_{10} is on the order of 10^{-4}, and obtained a value of 2×10^{11}, which is much smaller than the experimental value of $\sim 10^{16}$.

Our result, $P_{26,25}$, tends to confirm Montroll and Shuler's assumption of low transfer probability, because harmonic-oscillator theory predicts that transfer probability increases linearly with ν, giving $P_{10} = P_{26,25}/26 = 1/260$. The small value of A obtained from Eq. (C-32) may be due to the assumption in its derivation that collisions may transfer molecules only to the nearest adjacent vibrational levels.

Some comment on this selection rule for transfer by collision is in order. There seems to be some discrepancy among the various observations[8,17,49,5(] on the transfer directly from $\nu' = 26$ to 28 or $\Delta\nu' = +2$. In particular, those workers[8] who used a water-cooled mercury lamp emitting sharp lines did not observed fluorescence from $\nu' = 28$. Our observations show that lines from lamps that are not water-cooled (AH-4 and AH-2), even at one-fourth operating current and when cooled by an airblast, would be sufficiently broad to overlap the positions of both the 26'—0" and the 28'— 0" lines as given by Wood.[4] Thus the experiments[8,17,49,50] are

interpreted as showing equal probability for collision-induced transitions from $v' = 26$ for $\Delta v = +1, -1$ and -2.

It would be interesting to measure these transition probabilities from the $v' = 26$ level at higher temperatures, and from the $v' \cong 50$ level excited by the Cd-5086 line both at room and higher temperatures.

D. ACKNOWLEDGMENTS

I am deeply grateful to Professor Leo Brewer for directing my graduate research training and for guiding this work. I am grateful also to the many other people whose suggestions and comments have enriched my stay here.

Professor Francis A. Jenkins has graciously lent the Fabry-Perot interferometer and associated equipment and has discussed with me the single-line absorption measurements. Both he and Professor John G. Phillips have made available their microdensitometers. Messrs. C. A. McDowell and A. Arnot have supplied their unpublished data on the iodine fluorescence intensities. Mrs. Jane Waite has greatly expedited many phases of this research.

I wish to acknowledge also interesting discussions with Professors J. H. Hildebrand and R. S. Mulliken.

This work was done under the auspices of the National Science Foundation during the academic years 1956-59, and of the U. S. Atomic Energy Commission.

BIBLIOGRAPHY

1. L. Mathieson and A. L. G. Rees, J. Chem. Phys. 25, 753 (1956).

2. P. B. V. Haranath and P. T. Rao, J. Mol Spectr. 2, 436 (1958).

3. F. W. Loomis, Bull Nat. Research Council (U.S.) 11, 272 (1926).

4. R. W. Wood, (plate) Phil. Mag. 32, 329 (1916).

5. K. S. Pitzer and L. Brewer, Thermodynamics (McGraw-Hill, New York, to be published).

6. O. Stern and M. Volmer, Physik. Z. 20, 183 (1919).

7. B. Stevens, Can. J. Chem. 37, 831 (1959).

8. C. Arnot and C. A. McDowell, Can. J. Chem. 36, 114, 1322 (1958).

9. O. K. Rice, J. Chem. Phys. 9, 258 (1940).

10. R. C. Tolman, Phys. Rev. 23, 693 (1924).

11. C. Füchtbauer, Physik. Z. 21, 322 (1922).

12. W. Luck, Z. Naturforsch. 7a, 823 (1952), ibid. 6a, 313 (1951).

13. C. Malamond and H. Boiteux, Compt. Rend. 238, 778 (1954).

14. H. H. Hupfeld, Z. Physik 54, 484 (1929).

15. P. Pringsheim, Fluorescence and Phosphorescence (Interscience, New York, 1949).

16. E. Rabinowitch and W. C. Wood, J. Chem. Phys. 4, 358 (1936).

17. J. C. Polanyi, Can. J. Chem. 36, 127 (1958).

18. O. Heil, Z. Physik 74, 18 (1932).

19. R. S. Mulliken, J. Chem. Phys. 8, 234 (1940).

20. Ibid, 57, 500 (1940).

21. E. Rabinowitch and W. C. Wood, Trans. Faraday Soc. 32, 540 (1936).

22. P. Sulzer and K. Wieland, Helv. Phys. Acta 25, 653 (1952).

23. V. Kondratjew and Z. Polak, Physik Z. Sowjetunion 4, 764 (1933).

24. F. W. Loomis and H. Q. Fuller, Phys. Rev. 39, 180 (1932).

25. F. G. Dlugosch: unpublished dissertation, Breslau (1923), quoted by Kohler.[26]

26. J. F. Kohler, Phys. Rev. 44, 761 (1933).

27. J. Harding, Phil. Mag. 21, 773 (1936).

28. M. N. Alentsev, Doklady Akad. Nauk S.S.S.R. 62, 607 (1948),Engl. trans. D. A. Fine.

29. D. R. Stull and G. C. Sinke, Thermodynamic Properties of the Elements, Advances in Chemistry Series 18, (American Chemical Society, Washington, D. C., 1956).

30. B. Rosen, Données Spectroscopiques (Hermann et Cie, Paris, 1951).

31. E. F. M. van der Held, Z. Physik. 70, 508 (1931).

32. A. G. Gaydon and R. W. B. Pearse, Proc. Roy. Soc. 173,37 (1939). See also A. G. Gaydon, Dissociation Energies (Chapman and Hall, Ltd., London, 1953).

33. O. Oldenberg, Z. Physik 45, 451 (1927).

34. D. H. Rank, J. Opt. Sco. Amer. 36, 239 (1946).

35. L. Pauling and E. B. Wilson, Jr., Introduction to Quantum Mechanics (McGraw-Hill, New York, 1935).

36. R. Minkowski, Z. Physik 36, 839 (1926).

37. A. C. G. Mitchell and M. W. Zemansky, Resonance Radiation and Excited Atoms (Cambridge University Press, London, 1934).

38. M. H. Davis, Thesis, California Institute of Technology, Pasadena, California, 1955. G. D. Bell, M. H. Davis, R. B. King, and P. M. Routly, Astrophys. J. 127, 775 (1958).

39. W. Schutz, Z. Astrophys. 1, 300 (1930).

40. Kavanaugh, Bjornerud, and Penner, J. Opt. Soc. Amer. 43, 380 (1953).

41. W. M. Elsasser, Phys. Rev. 54, 126 (1938).

42. S. S. Penner and R. W. Kavanaugh, J. Opt. Soc. Amer. 43, 385 (1953).

43. G. Herzberg, Spectra of Diatomic Molecules, Second ed., Van Nostrand, New York, 1950.

44. A. Michels, H. de Kluiver, and D. Middelkoop, Physica 24, 543 (1958).

45. R. S. Mulliken and C. A. Rieke, Repts. Progr. Phys. 8, 231 (1941).

46. L. A. Turner, Z. Physik. 65, 480 (1930).

47. Richard G. Brewer, I. A Method for Determining Radiative Lifetimes of High-Temperature Molecules. II. The Probability of Spontaneous Nuclear Reaction in Molecular Hydrogen, UCRL-8387, July 21, 1958.

48. J. Franck and R. W. Wood, Verhandl. Deut. Physik. Ges. 13, 78 (1911); Phil. Mag. 21, 314 (1911).

49. M. Eliaschevich, Phys. Rev. 39, 532 (1932); Physik Z. Sowjetunion 1, 510 (1932).

50. F. Rössler, Z. Physik 96, 251 (1935).

51. R. J. Dwyer, J. Chem. Phys. 7, 40 (1939).

52. E. Durand, J. Chem. Phys. 8, 46 (1940).

53. S. Pienkowksi, Acta Phys. Polon. 5, 127 (1938).

54. E. W. Montroll and K. E. Shuler, Advances in Chemical Physics, I. Prigogine, ed., (Interscience, New York, 1958).

APPENDIX: DESCRIPTION OF ELECTRONIC SYSTEM

Jerry M. Sakai and Fred E. Stafford

Introduction

This system (Fig. 1) measures the phase difference (from 2 to 90 deg) between two modulated light signals (5.206 Mc) to a minimum accuracy of 10%. The signals result from observing a modulated light beam at two points. The phase difference to be measured results from substituting a fluorescent sample for a reflecting sample at one of the observation points.

Photomultiplier tubes convert the modulated light to 5 Mc electrical signals. The radiofrequency (rf) signal is heterodyned down to 1 kc in a mixer where the mixing signal is generated by a crystal-controlled rf oscillator. Although frequency is translated, the phase information is preserved. The frequency difference or beat frequency is held constant to $\pm$ 0.1 cps by an automatic frequency control (AFC). The AFC uses tuning-fork-controlled k-kc oscillator as a frequency standard.

The signals -- called the "reference," and "phase-shifted" or "sample" signals -- are amplified in their respective channels. Both signals are fed into a phase detector driving a null meter. A null is indicated only when the incoming signals are 90 deg out of phase. For the purpose of obtaining a null with different phase shifts, calibrated, variable-phase shifters are included in each channel.

Phase measurements are made at 1 kc instead of at 5 Mc to reduce the effects of stray capacity on the accuracy of the RC phase shifter. Another advantage of the reduced frequency is the relative ease of obtaining a narrow band filter, i.e., a bandwidth of 100 cps at 1 kc represents a $Q = 10$, whereas at 5 Mc the Q would have to equal 50,000.

A lifetime measurement of a sample is accomplished by nulling the phase detector first with a reflecting sol, then with the fluorescent sample. The difference in phase settings for the two conditions is the desired phase angle. The lifetime, τ, is obtained by using the relation $\tan \phi = \omega\tau$, where ϕ is the phase difference and $\omega = 2\pi f$, f being the modulating frequency.

Photomultiplier Assembly and Sample Preamplifier

The photomultiplier assembly consisting of a photomultiplier tube (pm) and an output cathode follower (V1 or V2) is shown in Figs. 1, 3, and 4. Its purpose is to convert a light signal modulated at 5.206 Mc to an electrical signal of the same frequency. There are two identical assemblies in the system: one receives part of the light beam reflected by a $BaSO_4$ sol, and the other receives light from the fluorescent sample.* The latter photomultiplier with its associated circuitry is called the sample channel and the former the reference.

A cathode follower (cf) with a tuned circuit across its input is employed as an impedance matching device -- a high-input impedance with a low-output impedance. This prevents the signal-carrying coaxial cable† from loading the photomultiplier. The cathode-follower bandwidth is 200 kc and the gain equals 0.5. The output signal level at the reference photomultiplier is nominally 50 mv peak to peak (p.p.), whereas, the sample output varies from 50 mv down to 100 μv, depending on the type of sample. Signals from the reference photomultiplier are

---

*The light source, lenses, modulator, and oscillator are described in more detail in Part IB, Description of the Apparatus.

†However, it is necessary to use the cathode-follower-connected bias as shown in the schematic because the tube bias voltage is developed across the 93-ohm load.

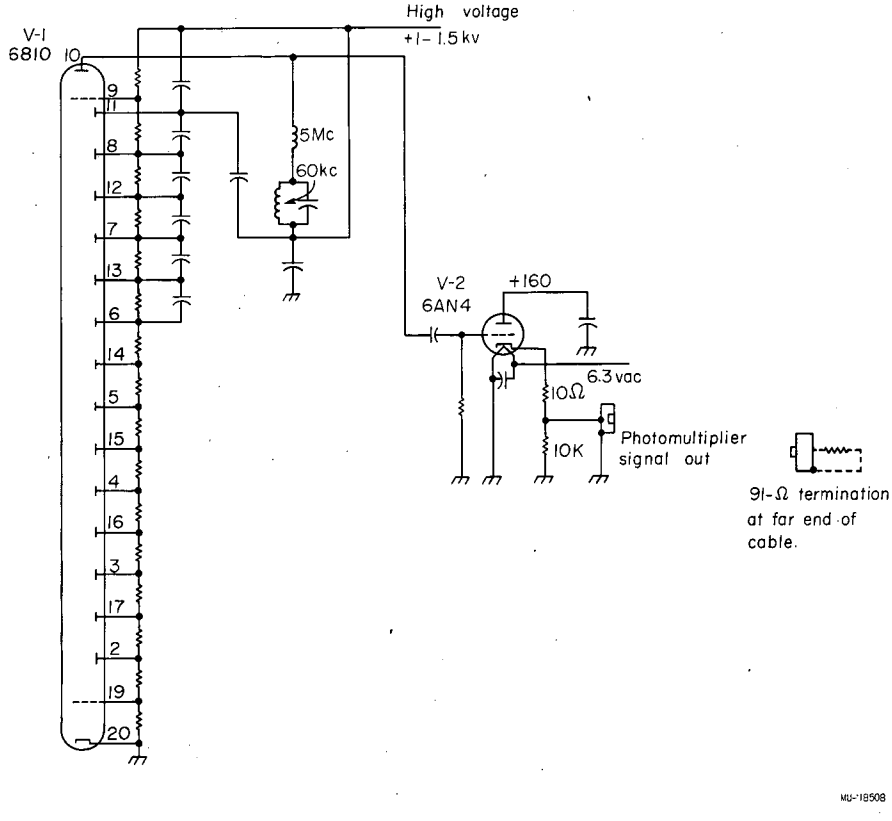

Fig. 3. Photomultiplier assembly.

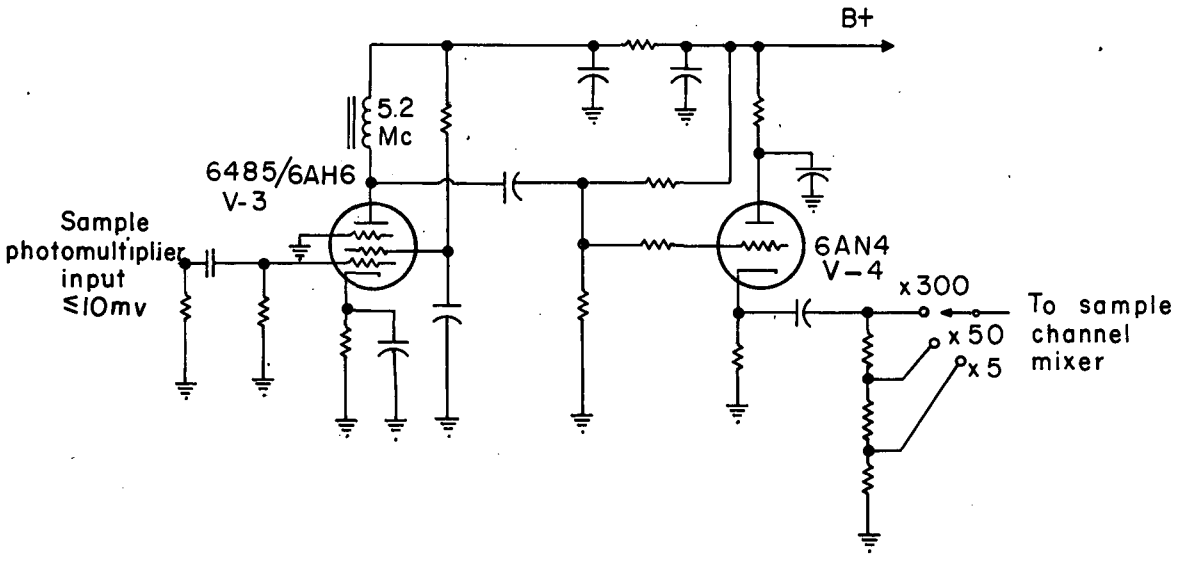

Fig. 4. The 5.2-Mc preamplifier.

fed directly into a mixer. However, sample outputs are preamplified to provide at least 20 mv at the input of the mixer.

The sample preamplifier* is a tuned amplifier (V-3) with a cathode-follower (V-4) output. The over-all gain is 300 with a bandwidth of 100 kc. In order to maximize the gain, the high-transconductance pentode† drives a high-impedance resonant circuit. Since the impedance at resonance is ωLQ, where ω is the radian frequency, Q the quality factor, and L the inductance, one uses the largest inductance permitted by the output capacity of the amplifier and the input capacity of the following stage. A cathode follower minimizes the effective shunt capacity across the coil by isolating it from the following cable and mixer input.

The reference mixer requires an input of at least 30 mv p.p. in order to supply adequate signal for the AFC to function effectively. For the 1-kc component, the gain of the mixer equals 4.

Mixer

The mixer (V8 or V19) translates the frequency of an incoming signal without loss of phase information (see Fig. 5). Mixing, or heterodyning, requires two signals of different frequencies. With the pentagrid mixer the resultant output consists of a Fourier series of components.

---

*Although the pre-amplifier is not part of the photomultiplier assembly, it is discussed to present the entire system up to the mixers.

†The gain equals $g_m Z_L$, where g_m is the transconductance and Z_L is the load impedance.

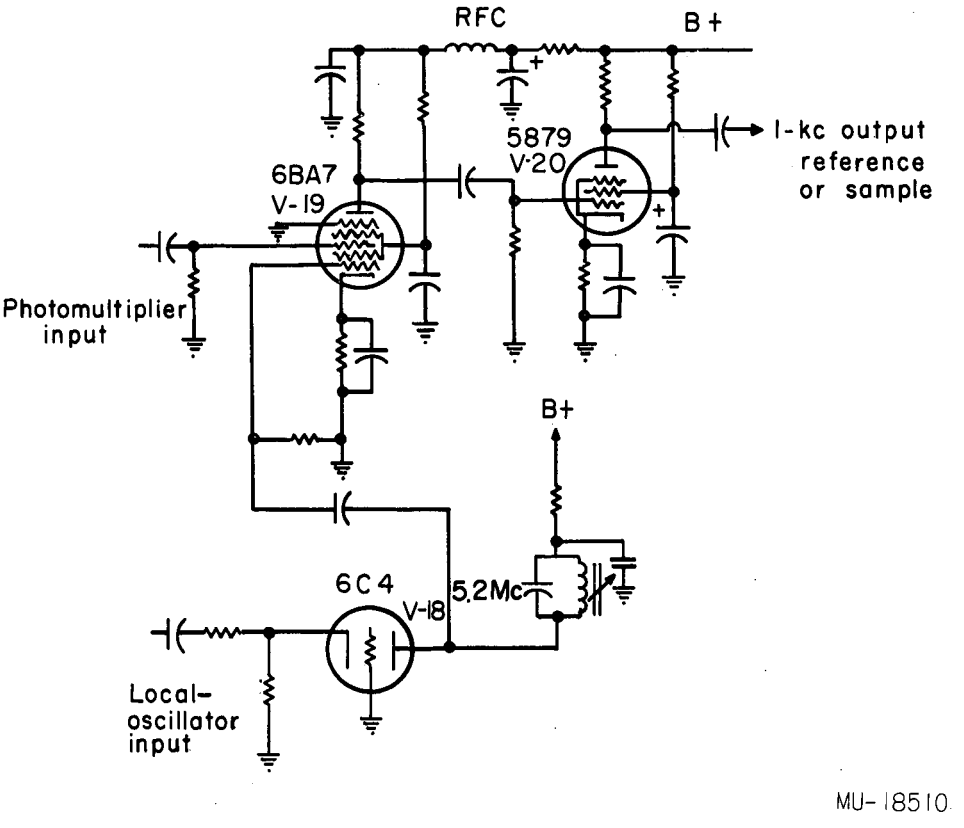

Fig. 5. Mixer, amplifier and grounded-grid amplifier.

In this system, only the difference frequency (1 kc) is used, and the remainder is filtered out. One of the two signals is generated by the local oscillator (beat oscillator), and the other is the photomultiplier output.

The pentagrid mixer operates according to

$$e_o = i_p R_L \simeq g_m' e_s R_L, \qquad (1)$$

where

e_o is the mixer output,

$e_s = A \cos \omega_s t$ is the photomultiplier signal,

R_L is the mixer load resistance,

i_p is the instantaneous plate current, and

g_m' is the instantaneous transconductance.

The transconductance is a function of the magnitude of the local oscillator signal and can be represented by a Fourier series:

$$g_m' = a_o + a_1 \cos \omega_o t + a_2 \cos 2\omega_o t + - - - - \qquad (2)$$

where $\omega_o/2\pi$ is the local oscillator frequency. The plate current can be written in the series form

$$i_p = A \cos \omega_s t \quad [a_o + a_1 \cos \omega_o t + a_2 \cos 2\omega_o t + - - - -] \qquad (3)$$

and when transformed

$$i_p = a_o A \cos \omega_s t + \frac{a_1}{2} A \cos(\omega_s - \omega_o)t + \frac{a_1}{2} A \cos (\omega_s + \omega_o)t + - - - \qquad (4)$$

The difference frequency term, $\frac{a_1}{2} A \cos (\omega_s - \omega_o)t$, appears without any phase shift, hence the phase is preserved through the mixer. Mixer gain depends on the frequency component of interest. The difference frequency gain is $\frac{a_1}{2} R_L$ where the value of a_1 can be determined only by graphical analysis of the transconductance curve. Frequently the Fourier coefficients,

a_i, are called the conversion transconductance.

The Automatic Frequency Control, Local Oscillator, and Isolation Amplifier

The automatic frequency control (AFC) shown in Figs. 6, 7, and 8 maintains the frequency difference between the photomultiplier signal and the beat oscillator output at 1 kc $\pm$ 0.1 cps by varying the beat oscillator frequency. A phase detector compares the phase of the output of the reference mixer (after it is amplified and filtered) with a standard 1-kc signal. The phase detector output is a dc signal proportional to the cosine of the phase difference of the incoming signals. It is zero at 90 deg and maximum at 0 deg (+) and 180 deg (-). It then is amplified by a dc amplifier (V-10) that varies the capacitance of a reactance diode in the oscillator tank circuit.* Furthermore, the dc amplifier provides a reverse bias for the diode to allow operation about the center of the frequency range. Because the variable capacitor (reactance diode) influences the frequency of the beat oscillator, any frequency variation in the mixer output results in a frequency variation (of the opposite sign) at the output of the oscillator, thereby reducing the error that otherwise would be present. The variable capacitance diode is new to this version of the apparatus and replaces a variable screen-grid voltage control.

There is no steady-state error because the error signal is produced by a phase difference between the signals from the reference channel and the tuning fork standard. The average value of the frequency over a long

---

*Reverse bias changes diode capacitance by changing the width of the non-conducting volume (dielectric) of the diode.

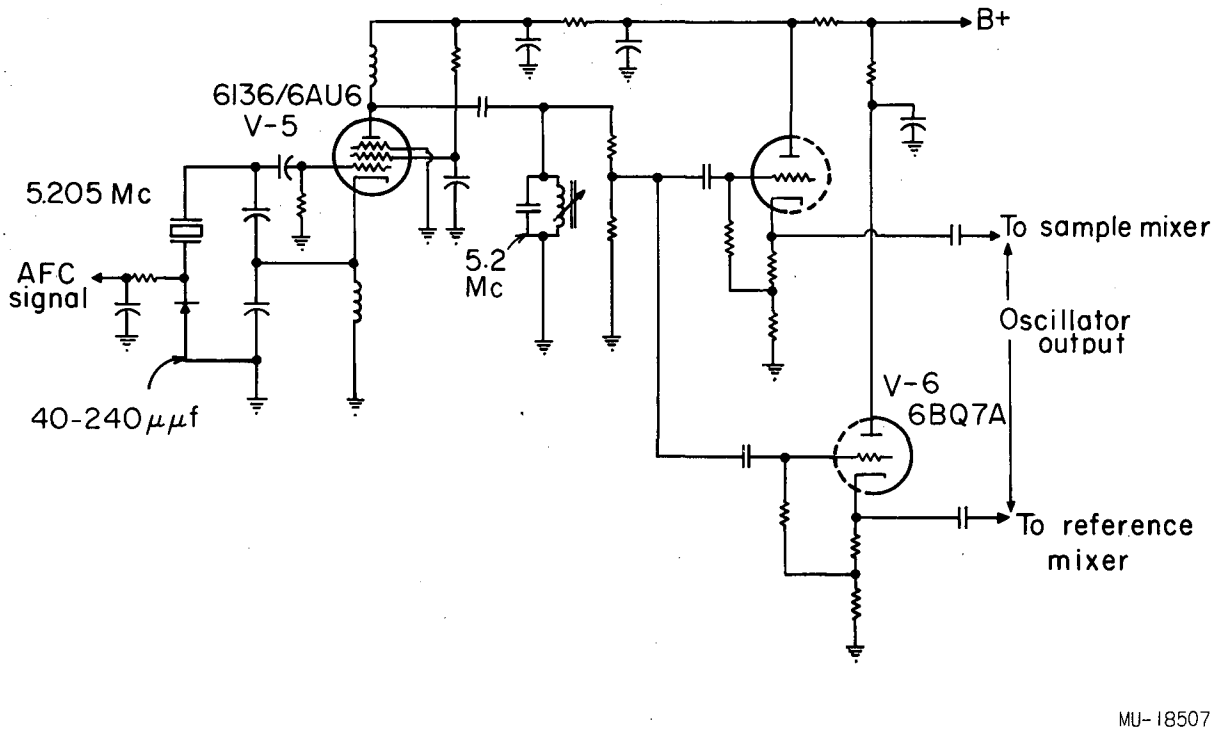

Fig. 6. Local oscillator

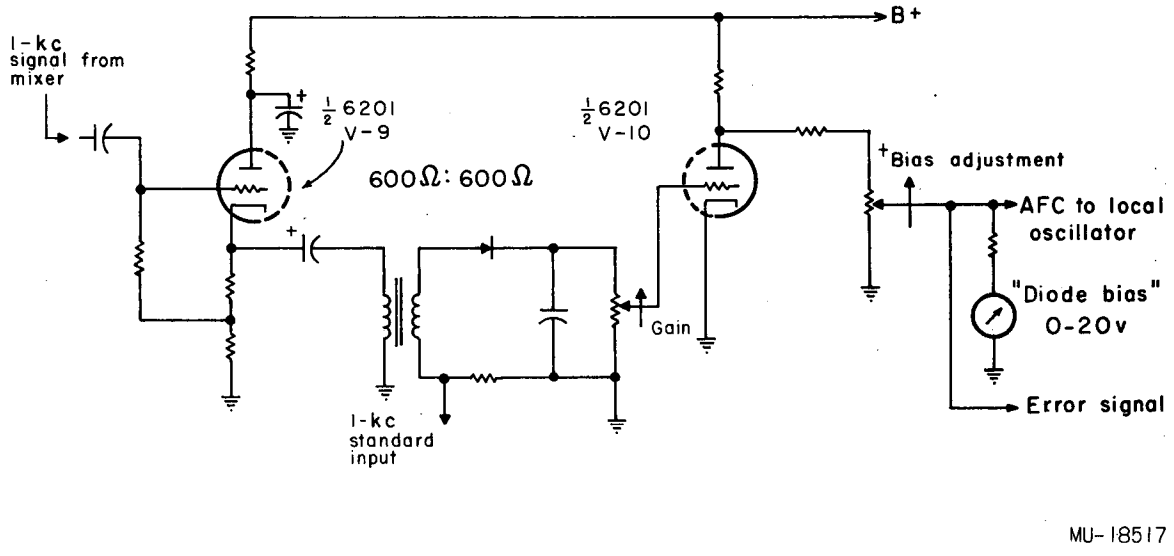

Fig. 7. Cathode follower, phase-detecting network, and dc amplifier.

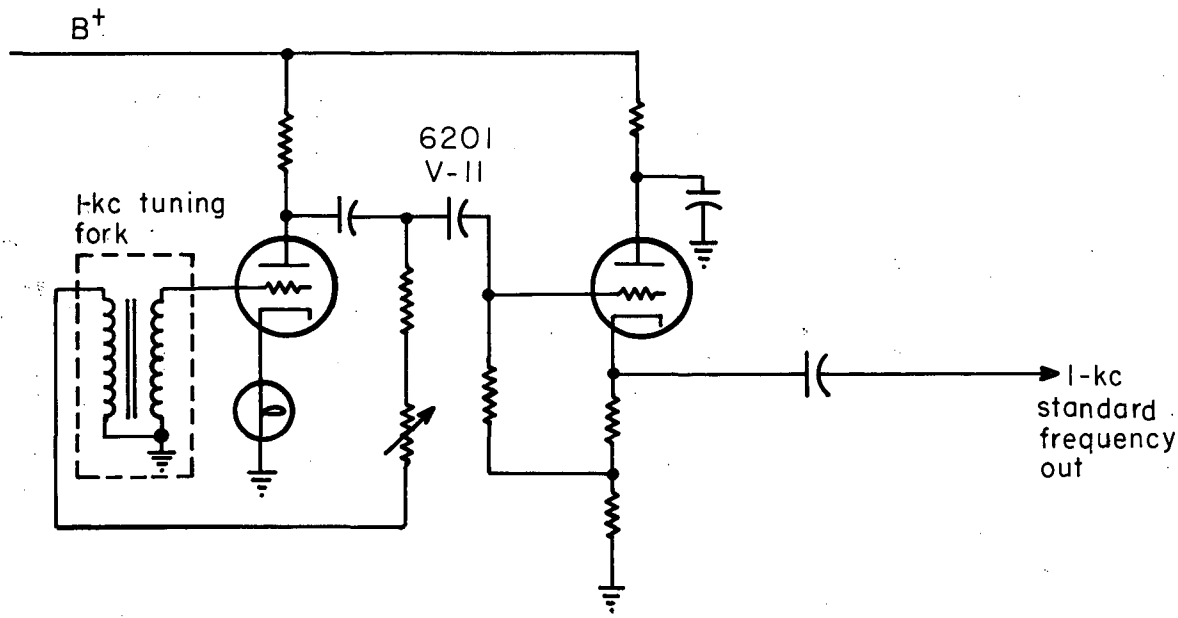

Fig. 8. Frequency standard

period of time is 1 kc $\pm$ 0.1 cps and is limited only by the stability of the tuning fork. Any transient fluctuation within the range of the AFC* is reduced by a factor equal to the loop gain, in this case approximately 100.

The standard is a 1-kc oscillator (V-11) which utilizes a tuning fork to determine the frequency. A 3-w, 120-v incandescent light bulb is in series with the cathode of the oscillator tube to provide bias and self-varying negative feedback. It is simply a resistor with an extremely large temperature coefficient. Its resistance increases with increasing current. The variable feedback insures good output waveform by preventing the tube from being overdriven. To minimize the loading on the oscillator by the low input impedance (600 ohms) of the phase detector, a cathode follower output is used.

In the phase detector, two signals -- the output and the standard -- are mixed and rectified. If the phase difference equals ϕ, then the output can be determined from the input as follows.

The input signals are $e_1 = E_1 \sin \omega t$ and $e_2 = E_2 \sin (\omega t + \phi)$. We set $E = E_1 = E_2$. Because the voltages are in series, they add vectorially:

$$e_1 + e_2 = E \left[\sin \omega t + \sin (\omega t + \phi)\right] \qquad (5)$$

$$= ZE \left[\sin (\omega t + \phi/2) \cos \phi/2\right] . \qquad (6)$$

The rectified, filtered output is proportional to the average value of $(e_1 + e_2)$ which is $\cos \phi/2$. It can be seen from this relation that as ϕ varies from 0 to 180 deg, the output goes from a maximum to a minimum.

---

*Errors or perturbations that are too fast (less than 1 msec) or too large (such as to cause saturation of the amplifier) will not be regulated out.

A variable-frequency Clapp oscillator (V-5) serves as the beat oscillator or local oscillator with nominal frequency f_L equal to 5,205,383 cps. The variable capacity causes a maximum positive frequency deviation of approximately 1000 cps for the maximum rated voltage change of 25 v on the diode (Fig. 6). This produces a capacity change from 40 uuf to 240 uuf. Electron coupling minimizes the interaction of the following stages with the oscillator. Tuning the plate tank circuit through its entire range causes a measured frequency shift of only 4 to 5 cps. The short-term stability with all external variables fixed (diode bias, tuning, etc.) is $\pm$ 1 cps.

The two outputs of the oscillator have separate cathode followers -- one output goes to the reference mixer and the other to the sample mixer. The interchannel coupling is reduced by the grounded-grid amplifiers (V7, V18) between the oscillator output and the mixer. The signal at the output of the amplifier is approximately 4 v p.p.

One-kilocycle Amplifiers and Phase Shifter

There are three stages of amplification at 1 kc (Figs. 9, 10, and 11) providing a maximum gain of 400. The first stage (V12,V20) has a gain of 10 and a bandwidth of 125 cps. The cathode follower after the tuned amplifier prevents loading of the tuned circuit and permits use of a low-impedance gain-control potentiometer. The following two stages have a total gain of 40 and a 3-kc bandwidth. The gain control should be adjusted so that the signal level at this point is approximately 15 v p.p. This results in a signal of 12-v p.p. at the output to the oscilloscope.

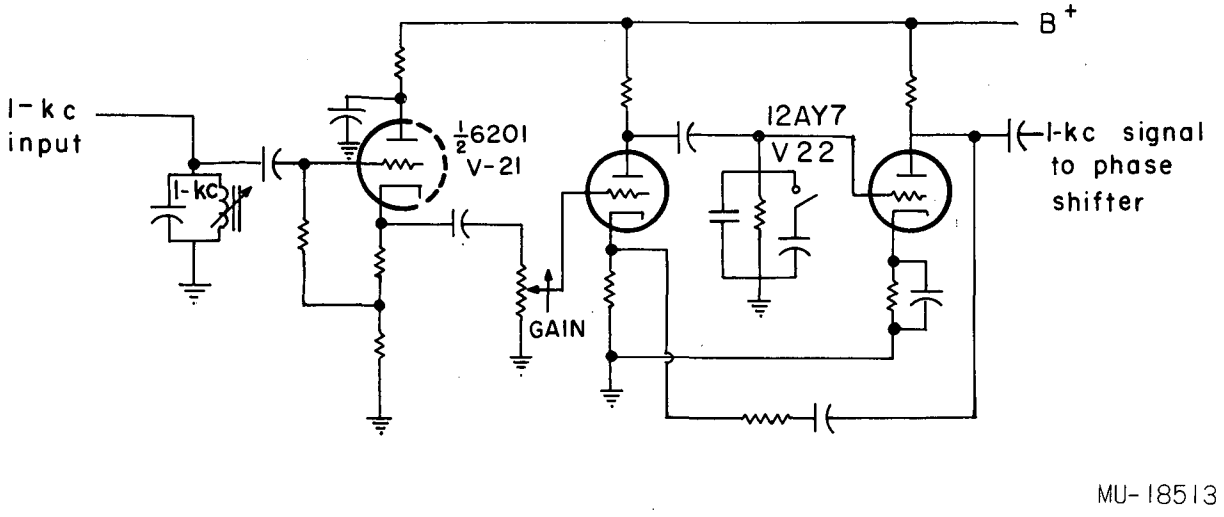

Fig. 9. One-kilocycle amplifiers.

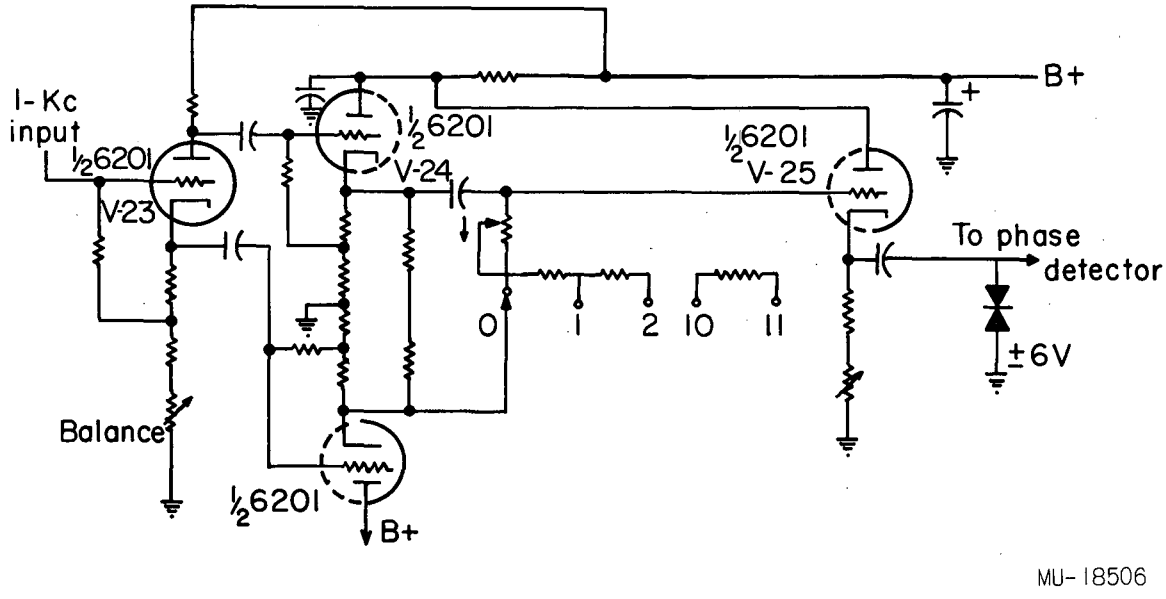

Fig. 10. Calibrated phase shifter.

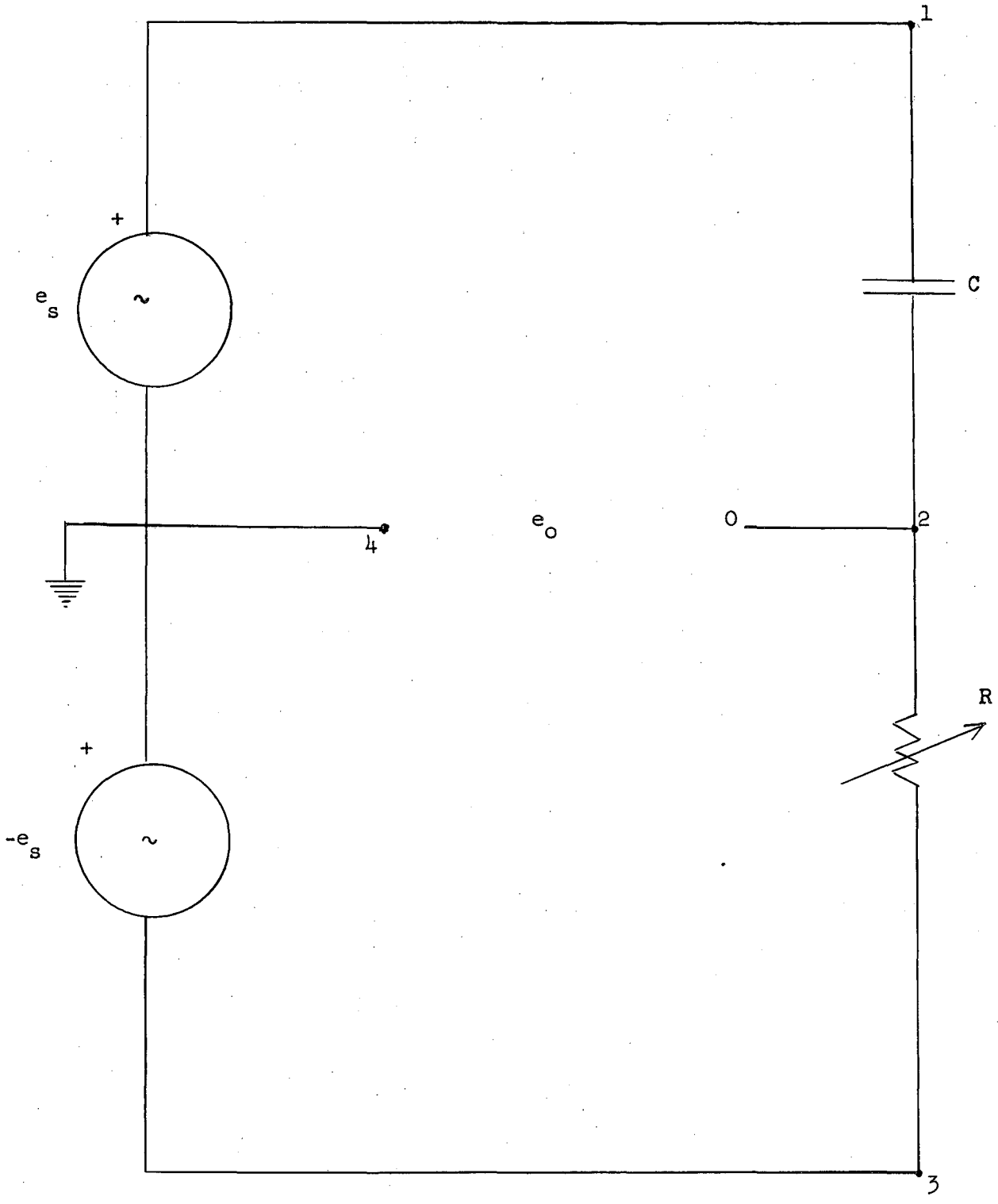

e_s, $-e_s$ = input

e_o = output (phase shifted)

Fig. 11. Equivalent circuit of phase shifter.

The phase shifter consists of a balanced signal input to an RC network. A phase inverter (V15, V23) provides the balanced signal by splitting the original signal into two equal components, 180 deg out of phase with respect to each other. It is necessary that the signals impressed across the resistor and capacitor be exactly equal in magnitude with respect to ground. To insure this, a potentiometer (Bal. 1) is inserted in the cathode of the phase detector to adjust the signal level until a minimum appears at the scope output. Each signal then drives a cathode follower (V16, V24) which in turn applies a signal across a capacitor in series with a variable resistor. The output signal appears between RC and ground as shown in Fig. 11.

The phase-shifter dial reads directly in ohms, i.e., the resistance is 900 ohms per step on the switch and 1000 ohms maximum on the "Duodial." Frequency and capacity are fixed so that $\omega C = 10^{-4}$.

A typical reading might be:

Switch position = 5

Duodial setting = 693

Total resistance = 5 x 900 + 693 = 5193 ohms,

so that $\tan \phi/2 = \omega RC = 0.519$.

The resistors and capacitors used in the phase shifter have been measured to an absolute accuracy of 0.1% and have a temperature coefficient of 20 parts per million per degree C. Stray capacity, largely due to the input and output capacity of the vacuum tubes, is of the order of 10 uuf (estimated) and the inductance of a 1-k wirewound resistor is 3 μh. The effect of the inductance and the capacitance is less than 0.1% under any circumstance. The over-all accuracy of the phase shifter is $\pm$ 0.1% or 0.1°, whichever is greater.

A cathode follower (V17A, V25) at the output of the phase shifter minimizes the loading across the RC network. At the same time it offers a low internal impedance source to drive the phase detector. At the output of the cathode follower, a double 6.5-v zener* diode clips the signal to reduce amplitude variations. The clipped signal is constant in amplitude at approximately 13 v p.p.

An equivalent circuit for the phase shifter is shown in Fig. 11. The potential, e_o, at 2 with respect to ground can be expressed as

$$e_o = -e_s + 2e_s \left(\frac{R}{R - j/\omega c} \right) \tag{7a}$$

$$= e_s \frac{(R + j/\omega c)}{(R - j/\omega c)} \,. \tag{7b}$$

Clearing the denominator of the complex term by multiplying the numerator and denominator by the complex conjugate of the denominator, we obtain

$$E = \frac{E_o (R^2 - 1/\omega^2 c^2) + j(2R/\omega c)}{(R^2 + 1/\omega^2 c^2)} \tag{8}$$

which is of the form

$$E = E_o [x + jy] = A e^{j\theta} \tag{9}$$

where

$$A = | x + jy | = 1 = \left[\frac{R^2 + 1/\omega^2 c^2}{(R^2 + 1/\omega^2 c^2)^2} \right]^{1/2} \tag{10a}$$

---

*Effectively two diodes "back to back" with the zener region at 6.5 v in each unit.

$$\theta = \tan^{-1} (2 R \omega c)/(R^2\omega^2c^2 - 1) = \tan^{-1} y/x , \qquad (10b)$$

and, by the trigonometric identity

$$\tan 2x = (2 \tan x)/(\tan^2 x - 1) ,$$

$$(\theta/2) = \tan^{-1} \omega R c . \qquad (10c)$$

Thus, by Eq. (10a), the amplitude of the output remains constant as the phase shifter setting is varied. Equation (10c) may be used for determining θ.

Phase Detector

The phase detector shown in Fig. 12 produces an output that is proportional to the cosine of ξ, where ξ is the phase difference of the two input signals to the phase detector. Thus the output is zero when the input signals are 90 degrees out of phase and maximum at 0 and 180 degrees. The equivalent circuit is shown in Fig. 13. The input signals are $e_1 = E_1 \sin \omega t$, $-e_1 = -E_1 \sin \omega t$, and $e_2 = E_2 \sin (\omega t + \xi)$. At point A the voltage is the vector sum of e_1 and e_2 or, more correctly, e_1 and e_2 less the voltage drop across the series resistor (R_1 and R_2). Similarly, at point B, the voltage is the vector sum of e_1 and e_2 minus the drop across R_4 and R_5. Mathematically, it can be written as follows:

$$e_A = \sin \omega t + \sin (\omega t + \xi) = 2 \sin 1/2 (2 \omega t + \xi) \cos \xi/2 \qquad (11a)$$

$$e_B = -\sin \omega t + \sin (\omega t + \xi) = 2 \cos 1/2 (2 \omega t + \xi) \sin \xi/2 . \qquad (11b)$$

The voltages are rectified -- e_A by diode D1 and e_B by diode D2. The output, which appears across the resistors R_3 and R_6, is the vector difference of the rectified signals. Subtracting e_A from e_B we have

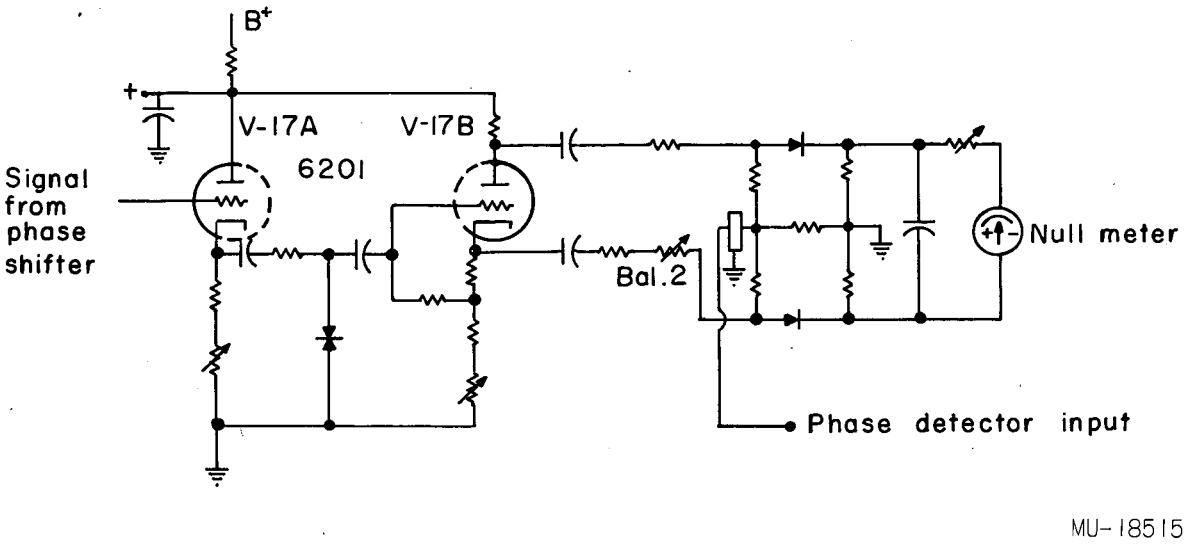

Fig. 12. Phase-detector circuit.

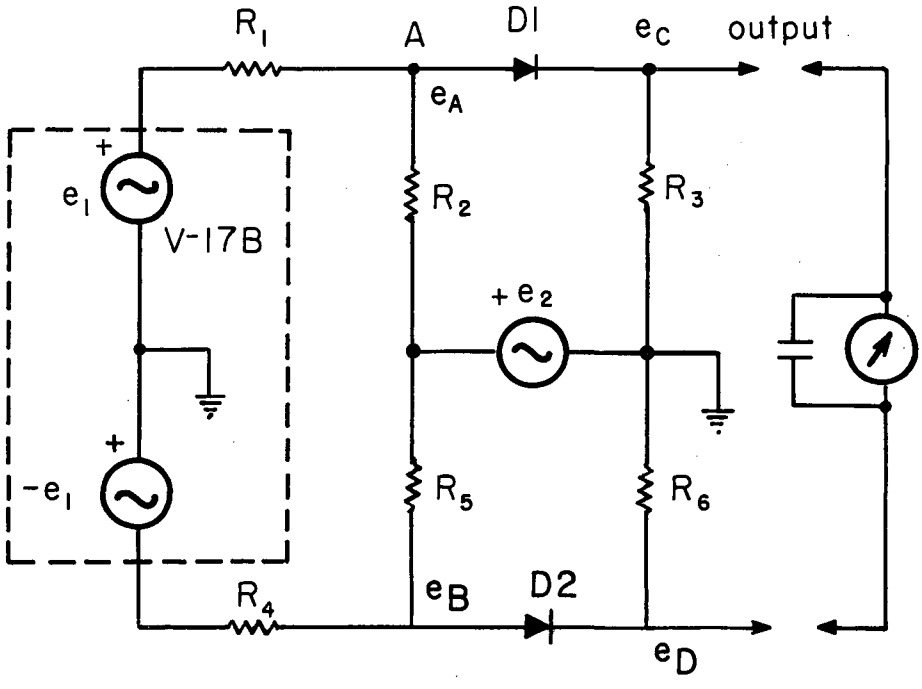

Fig. 13. Equivalent circuit of phase detector.

$$e_A - e_B = 2 [\sin (\omega t + \xi) \cos \xi/2 - \cos (\omega t + \xi/2) \sin \xi/2] \qquad (12a)$$

$$= \sin \omega t \cos^2 \xi/2 + \cos \omega t \sin \xi/2 \cos \xi/2 - \cos \omega t \cos \xi/2 - \sin \omega t \sin^2 \xi/2$$

$$= \sin \omega t \cos^2 \xi/2 - \sin \omega t \sin^2 \xi/2 = \sin \omega t (\cos^2 \xi/2 - \sin^2 \xi/2)$$

$$= (\cos \xi) \sin \omega t. \qquad (12b)$$

After the signal is rectified and filtered, the resulting dc voltage is proportional to cos ξ. The capacitor and the meter in parallel act as the filter.

When the inputs are 90 deg out of phase, the output is zero and, within the linear region of the tube, is independent of input amplitude. Consider the magnitudes of e_A and e_B in Fig. 13 when ξ = 90 deg. It can be seen that $| e_A | = | e_B |$; hence, we have $| e_C | = | e_D |$ and $| e_C | - | e_D | = 0$. Therefore, any amplitude disturbance at the input of the phase inverter which produces the same disturbance in both e_A and e_B is cancelled.

In reality, however, low frequency (less than 5 cps) perturbations upset the null. To reduce the effects of amplitude variations resulting from noise, the signals are clipped by 6-v Zener diodes* before entering the phase detector. A steady null is observed when the incoming signals are freed of amplitude variations in this way.

A source impedance-matching potentiometer is in series with the output from the cathode of the phase inverter (V-17b) to equalize the cathode and plate output impedances. The effect of unbalanced impedance can be seen by observing the null meter deflect as the input from the sample

---

*A diode whose Zener breakdown voltage is 6 volts. The diode conducts when the inverse voltage exceeds 6 v.

channel is varied over a small voltage range with no signal in this reference channel.

The output magnitudes of the phase inverter are adjusted to be equal by means of the Balance 2 (Bal 2) resistor. This is checked by using only the reference signal to obtain a null.

Because current increments on the order of 0.1 μa can be observed, the sensibility is approximately 0.2 deg. With clean signal input, this is the limiting sensibility of the instrument. However, under actual experimental conditions, input signals are very noisy, and the instrument sensibility is limited by "phase" noise reaching the detector.

Phase-Shift Test Oscillator

The purpose of the test oscillator (Figs. 14, 15, and 16) is to test the performance of the entire electronic system, independently of the optical systems. No similar means of testing had been used previously with this lifetime apparatus. Two outputs of the oscillator simulate the reference and sample photomultiplier outputs. Calibrated phase shifts of 0, 3, 20, and 70 deg. are included in the oscillator chassis corresponding to delay times of 0, 1.7, 11, and 40 μsec, respectively.

The test oscillator consists of a 2.603-Mc oscillator* (V-26), a frequency doubler, delay cables (in reference photomultiplier only) and two output cathode followers (V28, V29). The signal source is an electron-coupled, crystal-controlled, Colpitts oscillator with frequency doubling.

---

*There are two matched crystals used in this system -- one in the local oscillator, the other in the 2.6-Mc oscillator that drives the light modulator. The 2.6-Mc crystal is used in the test oscillator because the other is required for the operation of the electronic system.

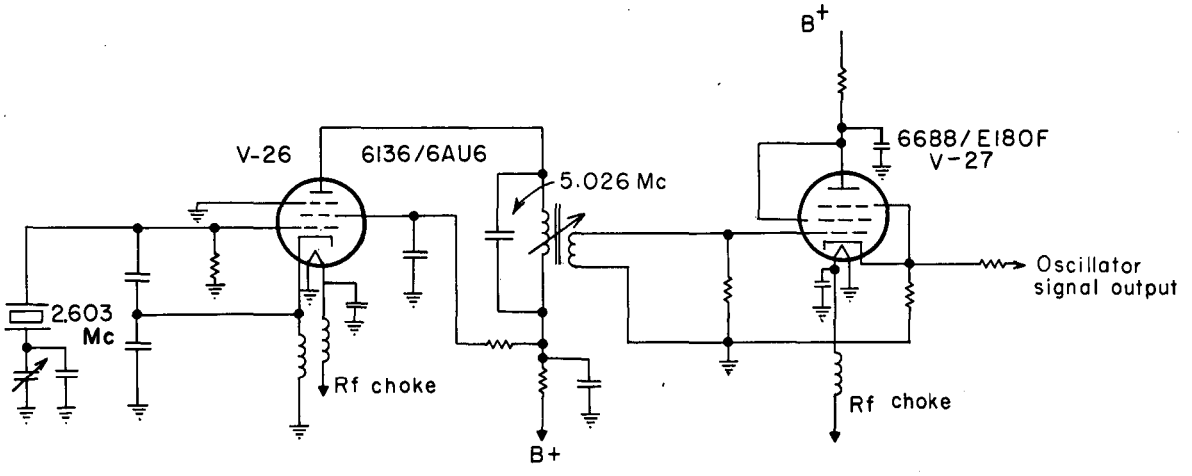

Fig. 14. Phase-shift test oscillator and doubler (f_c=5.206 Mc).

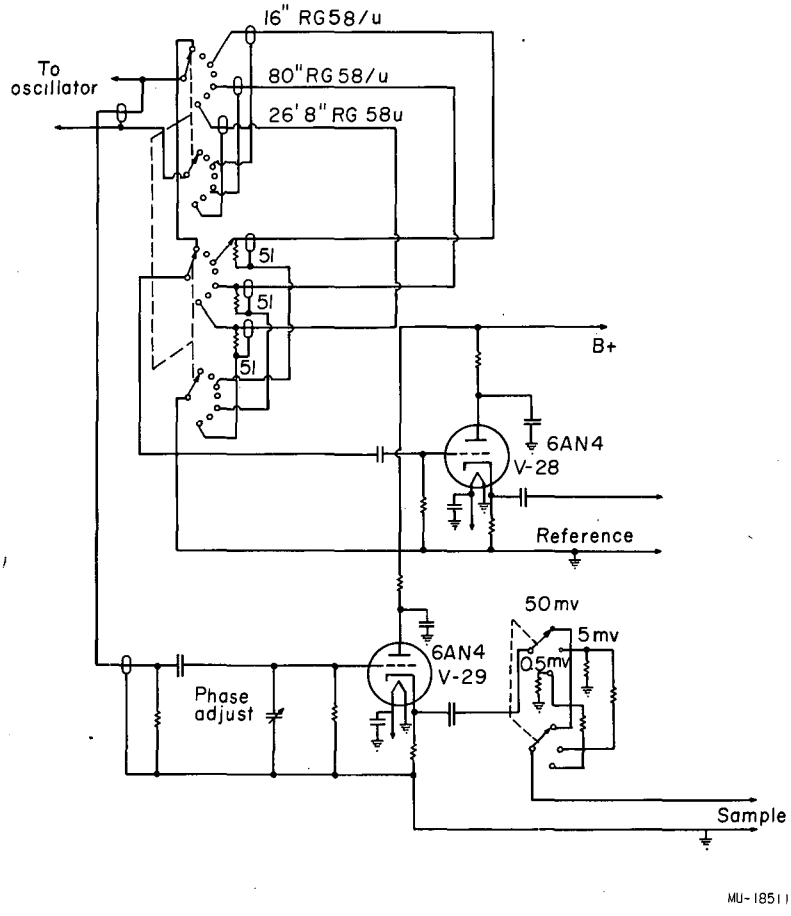

Fig. 15. Calibrated delay lines associated with phase-shift test oscillator.

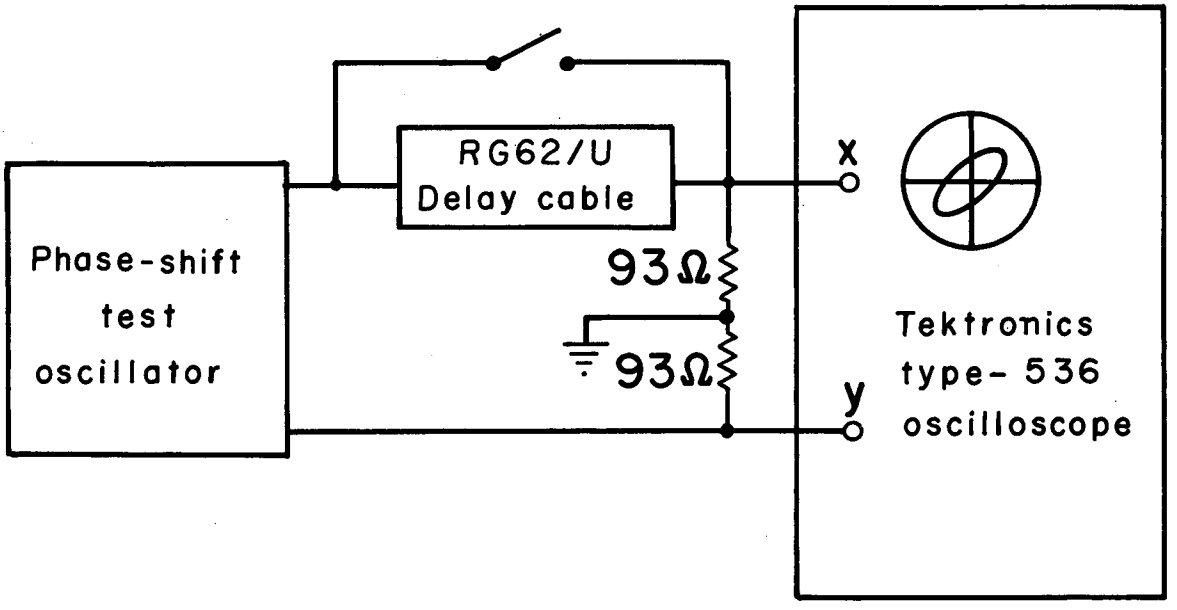

MU-18519

Fig. 16. Scheme for calibration of phase-shift test oscillator.

In the plate circuit of the oscillator, a tuned circuit, resonant at 5.206 Mc, acts as the doubling device by selecting the 5.2-Mc component of the oscillator output. A one-turn loop around the plate tank coil couples the signal (1 v p.p.) to the driver cathode follower (V-27). The output of the driver is split, where part of the signal goes to the reference output cathode follower (V28) through delay cables, and the other directly to the input of the sample cathode follower (V-29).

The phase shift results from having a delay cable in the reference transmission path. For a given length, the time delay in seconds is

$$t = v/d,$$

where v is the velocity of propagation in the cable in meters/sec (speed of light x propagation constant supplied by manufacturer) and d is the cable length in meters. The resultant phase shift in radians is

$$\phi = \omega t$$

where ω = frequency x 2π. Coaxial cable having a propagation constant of 0.69 (Type RG 58/U) is being used as the delay cable.

Both the outputs are 50 mv p.p. with a 93 ohm load.* In the "sample" channel there is an attenuator (x10, x100) to produce signal levels of 5 mv and 0.5 mv.

A variable capacitor is used across the input of the sample output cathode follower to adjust the phase at the "0" position.

The phase shifts were calibrated using external delay cables and a Tektronix type-536 oscilloscope with 53/54B vertical and horizontal

---

*The output is designed for use with terminated RG62/U cable. Other cable types will alter the signal level; however, if terminated, they will not affect the phase. Lengths up to 100 ft can be used with less than 3 db attenuation.

pre-amplifiers as in Fig. 16. The oscilloscope was trimmed to present a diagonal line (Lissajous pattern for 0 deg.) for the zero phase-shift position, and then the reference signal was shifted in phase. Cable was inserted into the external transmission line on the sample side until the Lissajous pattern closed. The length of cable was measured and the phase shift was computed. The zero-phase pattern on the oscilloscope was discernable to approximately 0.01 radians or 0.57 deg. The external cable (RG62/U) propagation constant (0.84) was known to within 5%. Coaxial cable was used to calibrate the phase because other techniques were not readily available.* Those available, such as determining the phase from a Lissajous pattern directly, were not as accurate. The Lissajous pattern for small angles (less than 10 deg) was measurable to within 30% of the total angle.

Discussion

The limitation of the system is the noise level for small signals, in that the sensibility of the null meter is frequently far less than the angle being measured. The noise-to-signal ratio at levels below 500 mv at the output of the photomultiplier assembly is not known. Measurements at this level, however, are difficult to make, if not impossible. Narrower bandwidths -- approximately 10 cps or less -- in the 1-kc channels would reduce the noise level to permit measurements for signal levels down to 100 mv. The spurious phase shift arising from a narrow-band filter would be largely eliminated if identical filters

---

*It should be noted that most techniques do not measure the phase of the two signals directly, but rather cable delays are measured.

were installed in both channels.* If both filters behave identically, any phase shift due to frequency variations will be cancelled. One way to obtain a narrow band is with a Q multiplier where bandwidths of 10 cps are easily obtainable with standard components.

The other limitations are the voltage gain available and the sensitivity of the phase detector. The gain is sufficient to amplify 100-mv signals (provided the noise can be filtered out). It can be increased without too much difficulty by a factor of 10 by adding another stage of rf amplification. In the limit, of course, the minimum measurable signal level is determined by the allowable bandwidth of the system. The phase-detector sensitivity is limited by the incoming signal amplitude, which in turn is limited by the linear range of the vacuum-tube phase inverter. At best, with the present circuit, the sensitivity can be increased a factor of 2 by increasing the signal level.

Summary

The purpose of the system is to measure phase differences ranging from 2 to 90 deg with a minimum accuracy of 10%. The sample channel can amplify signals as low as 500 uv to a level sufficient to permit measurements. The effective bandwidth in both channels (up to the phase detector) is 125 cps. For the reference channel, the optimum input signal level is 50 mv p.p. and the minimum is approximately 30 mv.

The mixer translates the frequency of the signal without introducing any phase shift. The AFC stabilizes the beat frequency to the precision

---

*However, the reference channel does not require additional filtering to eliminate noise.

of the tuning fork ($\pm$ 0.1 cps) on a long-term basis. Short-term frequency instability may exceed the above limits.

The phase shifter requires a balanced signal that should be checked and adjusted regularly. The phase shifter dials read directly in units of resistance. Resistance readings are converted to phase angles by the equation $\tan \frac{\theta}{2} = \omega C R = 10^{-4} R$. The phase shifter is accurate to within 0.1 deg or 0.2%, whichever is greater.

The phase detector indicates a null only when the input signals are 90 deg out of phase. Its sensitivity is 1.5 deg/μa at the null and the sensibility is 0.2 deg/μa for noise-free, clipped signals. The frequency response is about 5 cps -- approximately that of the null meter. The requirement for proper operation is a balanced output with equal source impedance from the plate side and the cathode side of the phase inverter.